Secondary aerosol formation promotes water uptake by organic-rich wildfire haze particles in Equatorial Asia

Jing Chen[1, *], Sri Hapsari Budisulistiorini[1], Takuma Miyakawa[2], Yuichi Komazaki[2], Mikinori Kuwata[1, 3, 4, *]

[1] {Earth Observatory of Singapore, Nanyang Technological University, Singapore, Singapore}

[2] {Research and Development Center for Global Change, Japan Agency for Marine-Earth Science and Technology, Yokosuka, Japan}

[3] {Asian School of Environment, Nanyang Technological University, Singapore, Singapore}

[4] {Campus for Research Excellence and Technological Enterprise (CREATE) program, Singapore, Singapore}

* Correspondence to: chen.jing@ntu.edu.sg; kuwata@ntu.edu.sg

For submission to

Atmospheric Chemistry and Physics

1   **Abstract**

2   The diameter growth factor (*GF*) of 100 nm haze particles at 85 % relative humidity and their

3   chemical characteristics were simultaneously monitored at Singapore in October 2015 during a

4   pervasive wildfire haze episode that was caused by peatland burning in Indonesia. Non-

5   refractory submicron particles (NR-PM$_1$) were dominated by organics (approximating 77.1 % in

6   total mass), whereas sulfate was the most abundant inorganic constituent (11.7 % on average). A

7   statistical analysis of the organic mass spectra showed that most organics (36.0 % of NR-PM$_1$

8   mass) were highly oxygenated. Diurnal variations of *GF*, number fractions of highly hygroscopic

9   mode particles, mass fractions of sulfate, and mass fractions of oxygenated organics (OOA)

10   synchronized well, peaking during the day. The mean hygroscopicity parameter (κ) of the haze

11   particles was 0.189 ± 0.087, and the mean κ values of organics were 0.157 ± 0.108 (κ_{org}, bulk

12   organics) and 0.266 ± 0.184 (κ_{OOA}, OOA), demonstrating the important roles of both sulfate and

13   highly oxygenated organics in the hygroscopic growth of organics-dominated wildfire haze

14   particles. κ_{org} correlated with the water-soluble organic fraction insignificantly, but it positively

15   correlated with f_{44} (fraction of the ion fragment at *m/z* 44 in total organics) ($R = 0.70$), implying

16   the oxygenation degree of organics could be more critical for the water uptake of organic

17   compounds. These results further suggest the importance of sulfate and secondary organic

18   aerosol formation in promoting the hygroscopic growth of wildfire haze particles. Further

19   detailed size-resolved as well as molecular-level chemical information about organics is

20   necessary for the profound exploration of water uptake by wildfire haze particles in Equatorial

21   Asia.

1. Introduction

In the last few decades, wildfire haze has periodically raged throughout equatorial Asian countries (Page et al., 2002; van der Werf et al., 2010; Field et al., 2016; Koplitz et al., 2016), resulting in billions of dollars of economic losses as well as thousands of premature deaths (Johnston et al., 2012; Marlier et al., 2013). The increasing wildfire activity is associated with the recent rapid change in land use for agricultural development, including industrial plantations over peatland (Page et al., 2009; Marlier et al., 2015; Spracklen et al., 2015). Such developments are accompanied by the drainage of water of pristine peat swamp forest, making the tropical peatland susceptible to fire (Langner et al., 2007; Konecny et al., 2016). The occurrence of peatland fires is closely related to El Niño-induced droughts (Page et al., 2002; Field et al., 2016). Enhanced peatland fires have been observed during intense El Niño years, including 1997, 2006, and 2015 (Page et al., 2002; van der Werf et al., 2010; Stockwell et al., 2016). In 1997, the peatland fire was of global concern, as the total carbon emission was estimated to equal 13−40 % of the year's annual global carbon emission from fossil fuels (Page et al., 2002). The recent equatorial Asian wildfire haze event in 2015 could rival the one in 1997 not only in terms of the hazards to human health but also the significant impacts on global climate (Crippa et al, 2016; Field et al., 2016; Huijnen et al., 2016; Koplitz et al., 2016; Stockwell et al., 2016). During September−October 2015, thick smoke from peatland fires blanketed Equatorial Asia and released huge amounts of organic material and fine particulate matter (particulate matter of aerodynamic diameter below 2.5 μm, $PM_{2.5}$) (Crippa et al, 2016; Koplitz et al., 2016), which is the leading cause of global air-pollution-related mortality (Kunii et al., 2002; World Health Organization, 2009; Johnston et al., 2012; Marlier et al., 2013; Lelieveld et al., 2015).

A previous study on the peatland fire event in 1997 has reported that the wildfire haze particles resulted in dramatic cooling effects on the atmospheric radiative budget, especially over the source region of Indonesia (-150 W m^{-2}) and the tropical Indian Ocean (-10 W m^{-2}) (Duncan et al., 2003). In addition to the subsequently affected shallow warm clouds and deep convection processes, the resultant abnormal rainfall in adjacent tropical region and the extra-tropics was also confirmed by both satellite observations and model simulations (Rosenfeld, 1999). These studies demonstrate the importance of investigating aerosol-cloud-precipitation

interactions of Indonesian wildfire haze particles, including water uptake properties of aerosol particles.

Previous studies on water uptake properties of aerosol particles stemmed from Indonesian peatland fires are controversial. On one hand, laboratory studies have demonstrated that fresh Indonesian peat burning particles are weakly hygroscopic and almost inactive as cloud condensation nuclei (CCN) (Chand et al., 2005; Dusek et al., 2005; Chen et al., 2017). On the other hand, a field observation showed that the wildfire haze particles were highly hygroscopic during the 1997 Indonesian peatland fires (Gras et al., 1999). Such discrepancies impede reliable evaluations of the effects on regional and global climate changes driven by Indonesian wildfire haze particles (Lin et al., 2013; Reid et al., 2013). The cause of the discrepancies needs to be understood quantitatively in comparison with the chemical composition of particles.

Aerosol particles emitted from wildfires are a mixture of inorganic and organic compounds, which complicates their water uptake properties (Carrico et al., 2008, 2010; Petters et al., 2009; Hallar et al., 2013; Lathem et al., 2013). Water uptake properties of inorganic salts, such as ammonium sulfate and ammonium nitrate, are well known, yet the hygroscopic behavior of organic compounds or organic-inorganic mixtures is still difficult to predict due to the complex chemical composition of organics and the associated distinct affinity for water of a specific chemical constituent (Saxena et al., 1995; Gysel et al., 2004; Dinar et al., 2007; Petters and Kreidenweis, 2007; Carrico et al., 2010; Kristensen et al., 2012; Marsh et al., 2017). For instance, experimental and modeling studies have shown that the water uptake by water-soluble matter is governed by the inorganic fraction, whereas the hygroscopic properties of inorganics can be altered substantially by the presence of organics (Saxena et al., 1995; Dick et al., 2000). In general, with the increase in the organic fraction, the water uptake by wildfire particles has presented an overall decreasing trend (Mircea et al., 2005; Carrico et al., 2010), evidencing the high sensitivity of particle water uptake to organic fractions. The high sensitivity to organic fractions has been observed, as inorganic species are much more hygroscopic than most organic compounds. However, the roles of inorganic and organic species in water uptake by Indonesian peatland burning particles have rarely been investigated (Dusek et al., 2005; Chen et al., 2017).

1   Water uptake properties of organic compounds have also been demonstrated to be

2 important especially when the chemical composition of aerosol particles is dominated by

3 organics. Such cases have been frequently observed in particles emitted from wildfires (Petters et

4 al., 2009; Carrico et al., 2010; Cubison et al., 2011; Hallar et al., 2013; Chen et al., 2017). Both

5 theoretical and experimental studies demonstrated that water-soluble organic matter (WSOM)

6 plays the key role in determining the water uptake by organic compounds (Peng et al., 2001;

7 Gysel et al., 2004; Petters and Kreidenweis, 2007; Carrico et al., 2008; Petters et al., 2009;

8 Lathem et al., 2013; Chen et al., 2017). For instance, freshly emitted peat burning particles are

9 known to contain a small fraction of WSOM, which explains their limited hygroscopicity (Chen

10 et al., 2017). Chemical aging and oxidation of organic compounds in both gas and particle phases

11 could alter the water uptake properties of aerosol particles in a wildfire plume (Gras et al., 1999;

12 Petters et al., 2009; Rose et al., 2010; Cubison et al., 2011). These chemical processes in the

13 atmosphere enhance the fractions of highly oxygenated organics and polar species, which are

14 typically water soluble (Duplissy et al., 2008, 2011; Jimenez et al., 2009; Chang et al., 2010;

15 Massoli et al., 2010; Cubison et al., 2011; Cerully et al., 2015). Although such chemical

16 transformation and corresponding changes in hygroscopicity have been observed in wildfire

17 particles in both the laboratory and the field (Petters et al., 2009; Massoli et al., 2010; Rose et al.,

18 2010; Cubison et al., 2011; Duplissy et al., 2011), the importance of these processes for water

19 uptake properties has never been investigated for peatland burning particles in the equatorial

20 Asian region.

21   In this work, we investigated the relationships between water uptake properties and the

22 chemical composition of aerosol particles in a tropical peatland fire haze in October 2015 by

23 conducting atmospheric observations in Singapore. We quantified water uptake properties using

24 the Humidified Tandem Differential Mobility Analyzer (HTDMA). In parallel, particle chemical

25 composition was characterized in real-time using the Aerodyne Time of Flight-Aerosol Chemical

26 Speciation Monitor (ToF-ACSM). Furthermore, water-soluble organic carbon (WSOC) and

27 elemental carbon (EC) contents were quantified by an off-line analysis of ambient $PM_{2.5}$ filter

28 samples. The data from these measurements were combined to explore how the water uptake

29 properties of tropical peatland burning particles are regulated.

2. Observation

2.1. Field Campaign

The field observation was conducted at the campus of Nanyang Technological University (NTU), Singapore (1°20′41″ N, 103°40′53″ E) during October 2015. The campus is located 20 km away from the city center, and surrounded by a secondary tropical forest and grassland. The site is located 0.8 km away from a highway, and a petrochemical complex (Jurong Island) is located approximately 8 km south. In September−October 2015, the observation site encountered severe transboundary haze pollution that was caused by recurring Indonesian peatland fires, dominated by the smoldering combustion of underground organic-rich peat soils and mixed surface vegetation burning (Field et al., 2016; Page et al., 2009; Jayaranthe et al., 2017). Particles emitted from the wildfires had experienced for approximately 1−4 days atmospheric aging process before arriving at Singapore (Fig. S1).

The observation was performed in an air-conditioned room, with the room temperature maintained at 22 °C. A cyclone (URG-2000-30EN PM$_{2.5}$, URG) was employed for ambient aerosol sampling at a flow rate of 16.67 L min^{-1}. The inlet was fixed on the rooftop, which was located approximately 10 m above the ground. The sample air was split into several flows for measurements with different instruments after drying by diffusion dryers (the relative humidity, *RH*, of the sample flow was below 30 %). During the observation, particle number size distribution, chemical composition, and hygroscopic growth were monitored.

2.2. Particle water uptake measurements

Water uptake properties were measured using the HTDMA system (Chen et al., 2017). Briefly, the sampled particles were desiccated using a diffusion dryer (Model 42000, Brechtel Manufacturing, Inc.), and the resulting dry polydisperse particles were classified by the first differential mobility analyzer (DMA, Model 3081, TSI Inc.). The DMA selects particles of a specific mobility diameter (*D$_0$*), which was fixed at 100 nm during the observation. The classified particles were humidified to *RH* = 85 % using nafion tubings (MD-110-12S-4, Perma Pure) operated under a controlled *RH* condition. The particle residence time in the humidifier was approximately 10 seconds. The variation in *RH* was ± 0.5 % (peak to peak). The resulting size distribution of humidified particles was measured by the second DMA coupled with a

condensation particle counter (CPC, Model 3775, TSI Inc.). The diameter growth factor parameter, g, which is defined as the ratio of the particle diameter after humidification at a conditioned RH ($D_p(RH)$) to the initial dry size (D_0) (i.e., $g = D_P(RH)/D_0$), was calculated from the HTDMA data. Hygroscopicity parameter, κ, was derived from the corresponding g at a given RH and D_0 using the following equation (Petters and Kreidenweis, 2007):

$$\kappa = (g^3 - 1) \cdot \left(\frac{1}{RH} \cdot \exp\left(\frac{4\sigma_{s/a} \cdot M_w}{\rho_w \cdot R \cdot T \cdot D_0 \cdot g} \right) - 1 \right), \tag{1}$$

where $\sigma_{s/a}$ is the surface tension of the solution/air interface (0.0718 N m^{-1} at 25 °C), M_w and ρ_w are the molecular weight (0.018 kg mol^{-1}) and density of water (1×10^3 kg m^{-3}), respectively; R is the universal gas constant (8.31 J K^{-1} mol^{-1}), and T is the absolute temperature (298 K). The HTDMA calibration results with 150 nm ammonium sulfate particles are shown in Fig. S2, demonstrating the validity of our instrument. Further details about the HTDMA are available in Chen et al. (2017).

2.3. Aerosol chemical analysis

The ToF-ACSM (Aerodyne Inc.) was utilized to measure the chemical composition of non-refractory submicron particles (NR-PM$_1$), including organics (OA), sulfate (SO$_4^{2-}$), nitrate (NO$_3^-$), ammonium (NH$_4^+$), and chloride (Cl$^-$) (Fröhlich et al., 2013). The ToF-ACSM sampled particles that were desiccated by a nafion tubing. The organic mass spectra measured by the ToF-ACSM were analyzed in detail using the Multilinear Engine (ME-2 solver) software (Canonaco et al., 2013). Four specific types of OA were identified: hydrocarbon-like OA (HOA), peat burning OA (PBOA), non-peat biomass burning OA (briefly BBOA), and oxygenated OA (OOA). The HOA factor was mainly contributed by primary sources, such as the combustion emissions from fossil fuel (e.g., related to traffic, shipping, and industrial use), excluding the influence of biomass burning. The PBOA and BBOA factors were attributed to the long-range transport from Indonesian peatland fires, and the two OA factors were well separated. Details about the ToF-ACSM measurements and data analysis are provided in Budisulistiorini et al. (2018).

PM$_{2.5}$ filter samples for chemical analysis were also collected using filter holders (BGI Inc.). The samples were collected for 24 hours using 47 mm (diameter) quartz-fiber filters. The sampling started/ended at 08:00 local time (LT). The collected samples were analyzed for bulk OC, EC, and WSOC. All the quartz-fiber filters were prebaked at 900 ℃ for 3 hours before sampling, after which they were stored in a refrigerator (−20 ℃) until analysis. For each sampling, a back-up quartz-fiber filter was used to account for the potential influence of gas phase organic components on the particulate organics collected on the front quartz-fiber filter (Turpin et al., 1994). The method assumes that all the particulate OC is collected by the front filter, while the gas phase OC is collected equally on both front and back filters. Subtraction of the OC loading on the back filter (i.e., gas phase OC) from that on the front one allows quantification of particulate OC (i.e., corrected OC).

Concentrations of OC and EC were determined by thermal-optical reflectance analysis (Chow et al., 1993) using the Sunset Laboratory OC/EC Analyzer, following the IMPROVE-A protocol. WSOC was quantified with the Sievers 800 Total Organic Carbon (TOC) Analyzer following extraction of part of a filter sample (8 mm φ) by 10 ml of HPLC-grade water. An orbital shaker was operated for 21 hours for the extraction, and the subsequent solutions were filtered with syringe filters (pore size of 0.2 μm).

2.4. Particle number size distribution

Particle number size distributions were measured using a NanoScan SMPS Nanoparticle Sizer (NanoScan-SMPS, Model 3910, TSI Inc.) and an Optical Particle Sizer (OPS, Model 3330, TSI Inc.). The detected particle sizes ranged from 11.5−365.2 nm (NanoScan-SMPS) in mobility size and 0.3−10 μm (OPS) in optical size. Both instruments sampled particles desiccated by a diffusion dryer (Model 42000, Brechtel Manufacturing, Inc.). The time resolution of both instruments was 1 minute.

3. HTDMA data analysis

3.1. Classification of three hygroscopic modes

Figure 1 shows the HTDMA data averaged over the entire observation period. The mean normalized particle size distribution after humidification at 85 % RH has spanned a few different modes, reflecting mixing states of ambient wildfire haze particles observed at Singapore (Bougiatioti et al., 2016; Ogawa et al., 2016). For particles in a specific hygroscopic mode, i, with $g_{1,i} < GF < g_{2,i}$, the number fraction of this mode (nf_i) was derived from measured probability density function of g (i.e., $c(g, D_0)$) as $nf_i = \int_{g_{1,i}}^{g_{2,i}} c(\mathrm{g}, \mathrm{D}_0)\, dg$. The corresponding mean GF ($g_{mean,i}$) was calculated from $g_{mean,i} = \dfrac{1}{nf_i} \int_{g_{1,i}}^{g_{2,i}} g\ c(\mathrm{g}, \mathrm{D}_0)\, dg$ (Gysel et al., 2009). The equivalent values of κ for mode i were obtained from $g_{mean,i}$ using Eq. (1).

The observed 100 nm dry particles were categorized into the following three groups based on their hygroscopic properties at RH = 85 % (temporal variation of the multimodal size distribution patterns are shown in Fig. S3 of the supplementary material), facilitating the analysis of heterogeneity of particle chemical composition:

(1) Nearly non-hygroscopic or weakly hygroscopic particles ($0 \leq \kappa < 0.1$; $g < 1.15$): Particles are predominantly composed of black carbon (BC) and non-polar hydrocarbon-like organic compounds (Peng et al., 2001; Gysel et al., 2007; Kreidenweis et al., 2008).

(2) Moderately hygroscopic particles ($0.1 \leq \kappa < 0.2$; $1.15 \leq g < 1.27$): They could contain hygroscopic organics (e.g., carboxylic acids and levoglucosan) and/or mixtures of non-/less and more hydrophilic compounds (e.g., BC, fatty acids, and/or humic-like substances mixed with ammonium sulfate or levoglucosan-like species) (Peng et al., 2001; Chan and Chan., 2003; Gysel et al., 2004, 2007; Chan et al., 2005; Petters and Kreidenweis, 2007);

(3) More hygroscopic particles ($\kappa \geq 0.2$; $g \geq 1.27$): Aerosol particles contain inorganic salts as well as some more hygroscopic organic species such as multifunctional organic acids (Peng et al., 2001; Carrico et al., 2008; Duplissy et al., 2011; Ogawa et al., 2016).

In addition, the volume-weighted mean growth factor, GF, was also calculated using $c(g, D_0)$ (Gysel et al., 2009):

1    $GF = (\int_0^{\infty} g^3 \cdot c(g, D_0) \cdot dg)^{1/3}$.   (2)

2 *GF* was employed to calculate the mean values of κ, which facilitated the comparison with

3 chemical composition of aerosol particles.

4 **3.2. Effective κ of organic compounds (κ_{org})**

5   Water uptake properties of organic compounds were estimated using the Zdanovskii–

6 Stokes–Robinson (ZSR) mixing rule, employing the observed values of κ and chemical

7 composition as input parameters. The ZSR mixing rule assumes that water uptake by a mixture

8 of materials is additive of the water content retained by each chemical species (Stokes and

9 Robinson, 1966). The rule also assumes that the volume change in the mixing of species within

10 individual particles is almost negligible (Brechtel and Kreidenweis, 2000, Gysel et al., 2007;

11 Petters and Kreidenweis, 2007):

12 $$\kappa = \sum_i \kappa_i \cdot \varepsilon_i = \kappa_{SNA} \cdot \varepsilon_{SNA} + \kappa_{org} \cdot \varepsilon_{org} + \kappa_{EC} \cdot \varepsilon_{EC}$$
$$\Leftrightarrow \kappa_{org} = \frac{\kappa - \kappa_{SNA} \cdot \varepsilon_{SNA} - \kappa_{EC} \cdot \varepsilon_{EC}}{\varepsilon_{org}} \quad , \quad\quad\quad\quad\quad (3)$$

13 where κ_i and ε_i stand for the hygroscopicity parameter and the volume fraction of a specific

14 component i in dry particles, respectively. The subscript *SNA* represents the three major

15 inorganic constituents of sulfate, nitrate, and ammonium; *org* denotes organic species; *EC*

16 indicates elemental carbon.

17   Sulfate, ammonium, and nitrate were considered for inorganics, the majority of which

18 were contributed by sulfate (see Table 2). Other materials, such as sea salt and crustal elements,

19 were demonstrated to be neglected because they are relatively scarce in submicron wildfire haze

20 particles in Southeast Asia (Balasubramanian et al., 2003; Keywood et al., 2003; See et al., 2006;

21 Stockwell et al., 2016). Almost all the sulfate and nitrate were neutralized by ammonia, and these

22 three most abundant inorganic constituents were combined and assumed as ammonium sulfate

23 (i.e., $\varepsilon_{SNA} = \varepsilon_{SO4} + \varepsilon_{NO3} + \varepsilon_{NH4} \approx \varepsilon_{AS}$). Thus, the value of κ_{SNA} was considered to approximate the κ

24 value of ammonium sulfate under the condition when sulfate dominates inorganics (Gunthe et al.,

1 2009; Chang et al., 2010; Ogawa et al., 2016). The elemental carbon (EC) is known as non-

2 hygroscopic (i.e., $\kappa_{EC} \approx 0$).

3   Values of densities are required to compute ε_i from observed mass fractions. The mass

4 fraction is taken as the first-order approximation of the volume fraction, based on the hypothesis

5 that the bulk particle density is similar to the densities of individual compounds when volume

6 additivity is assumed (Kreidenweis et al., 2008; Gunthe et al., 2009; Hallquist et al., 2009). This

7 hypothesis has been demonstrated to be acceptable when particles are composed primarily of

8 organics and sulfate (Cross et al., 2007; King et al., 2007). The densities of ammonium sulfate

9 and EC were assumed to be 1.77 g cm^{-3} and 1.80 g cm^{-3}, respectively (Park et al., 2004; Bond

10 and Bergstrom, 2006). The density of organics is known to vary depending on their elemental

11 composition (Kuwata et al., 2012). The value was assumed as 1.40 g cm^{-3}, which is a typical

12 value for ambient organic aerosols (Hallquist et al., 2009).

13   The EC mass fraction of approximately 10.0 % in submicron wildfire haze particles was

14 utilized according to the time-averaged EC content in ambient PM$_{2.5}$ filter samples (see Table 2).

15 This assumption was based on the preconditions that the wildfire haze particles were

16 homogeneously mixed in varied sizes and that there was no significant difference between BC

17 and EC. It should be noted that some difference in chemical composition could have existed

18 between particles quantified by the ToF-ACSM (NR-PM$_1$) and HTDMA (100 nm). Although the

19 data obtained by these two techniques are frequently combined for detailed analysis (e.g.,

20 Whitehead et al., 2016), the difference in particle size range along with the particle mixing state

21 (Whitehead et al., 2014) can be a source of uncertainty for the following discussion in this work.

22 **3.3. κ of oxygenated organic compounds (κ_{OOA})**

23   As described in Sect. 2.3, organics were numerically segregated to HOA, PBOA, BBOA,

24 and OOA. The value of κ_{org} can be calculated by a linear combination of contributions from

25 segregated fractions (Petters and Kreidenweis, 2007; Chang et al., 2010):

26 $\kappa_{org} = \upsilon_{HOA} \cdot \kappa_{HOA} + \upsilon_{PBOA} \cdot \kappa_{PBOA} + \upsilon_{BBOA} \cdot \kappa_{BBOA} + \upsilon_{OOA} \cdot \kappa_{OOA}$,   (4)

27 where υ_i stands for the volume fraction of component i in all the organics.

Water uptake by a mixed particle is largely driven by the relative abundance of more or less hygroscopic component, and it is more sensitive to uncertainties in the hygroscopicity of more hygroscopic compounds than that of less hygroscopic compounds (Gysel et al., 2007). Hydrocarbon (-like) OA is known to be almost non-hygroscopic, leading to the estimation that the κ value of HOA is 0 (Gysel et al., 2007; Gunthe et al., 2009; Chang, et al., 2010). Water uptake by freshly emitted biomass burning particles is generally limited, especially compared with OOA (Carrico et al., 2010; Chang et al., 2010; Chen et al., 2017). Based on our previously measured κ results of fresh Indonesian peatland burning particles, an overall mean value of κ_{PBOA} = 0.04 was used for the fresh PBOA factor, and κ_{BBOA} = 0.06 was applied for the non-peat BBOA factor with mixed vegetation burning mainly of acacia and fern species (Chen et al., 2017). Under these assumptions, κ_{OOA} can be calculated by the following equation:

$$\kappa_{OOA} = (\kappa_{org} - \kappa_{PBOA} \cdot \upsilon_{PBOA} - \kappa_{BBOA} \cdot \upsilon_{BBOA}) / \upsilon_{OOA} . \tag{5}$$

The density of OOA/PBOA/BBOA is required to calculate $\upsilon_{OOA}/\upsilon_{PBOA}/\upsilon_{BBOA}$ using the ME-2 resolved corresponding mass concentration combined with the total volume concentration of the bulk OA derived from the ToF-ACSM observed OA mass. The density of oxygenated organics was assumed to be 1.50 g cm^{-3} (as summarized in Table 1), which is a typical value for carboxylic and multifunctional organic acids (Saxena et al., 1995; Peng et al., 2001; Gysel et al., 2004; Carrico et al., 2010; Ogawa et al., 2016). According to the reported average density for common dry smoke particles (i.e., $1.20 - 1.40$ g cm^{-3}; Reid et al., 2005), and considering the dominance of non-refractory organic material in fresh Indonesian peatland burning particles (Budisulistiorini et al., 2017), the densities of PBOA and non-peat BBOA were assumed to be 1.10 and 1.20 g cm^{-3}, respectively. Detailed information on the parameters utilized for the κ_{org} calculation is provided in Table 1.

4. Results

In this section, aerosol number size distribution (Figure 2), chemical composition (Figures 3 and 4), and hygroscopic properties of aerosol particles (Figure 5) are described in addition to diurnal variations in these data (Figure 6).

4.1 Number size distribution of wildfire haze particles

Figure 2a displays the time-averaged particle size distribution within the entire size range of 11.5 nm−10 µm measured by NanoScan-SMPS combined with OPS. The NanoScan-SMPS data were used for the fine particles (11.5–365.2 nm), and the overlapped size range of the OPS (338 nm size bin) was excluded from the analysis. The data in the remaining OPS size range (419 nm–10 µm) were combined with the fine particle data. The temporal average size distribution presented a unimodal structure, in which the number mode diameter was located around 100 nm. Particles in the range of 30–200 nm dominated the total particle number concentration, whereas particles larger than 600 nm accounted for a minor fraction (less than 4.0 % on average; Fig. S4 and Fig. S5). This result suggests that in Singapore, the wildfire haze particles were predominantly contributed by submicron particles, in line with the corresponding chemical characteristics obtained in previous studies (Balasubramanian et al., 2003; See et al., 2006).

Figure 2b shows the mean diurnal cycle of particle number size distribution. The growth of ultrafine particles was typically observed in the afternoon. The $dN/dlogD_p$ higher than 1.5×10^4 cm^{-3} was commonly observed in the 50–200 nm particle size range, while the $dN/dlogD_p$ of super micron particles seldom exceeded 1.0×10^3 cm^{-3}. The particle number concentration was high from 08:00–09:00 LT in the morning. The concentration increased again in the afternoon (about 14:00 LT), which lasted until midnight. The high concentration periods could have been caused by local traffic emissions and by secondary formation processes. Diurnal variations were also observed in the number concentrations of all particles.

Figure 2c depicts the mean diurnal variations of the corresponding total particle number and volume concentrations. The total number concentration started to increase after 07:00 LT until around 10:00 LT, and it reached the highest level after 14:00 LT. The particle number concentration was higher than 1.5×10^4 cm^{-3} before 19:00 LT. After that, the number concentration decreased gradually, reaching 1.2×10^4 cm^{-3} at midnight. Correspondingly, the aerosol volume concentration was higher than 50.0 µm^3 cm^{-3} during the day. The volume concentration decreased during the night, although it was still higher than 45.0 µm^3 cm^{-3}. These

1 results demonstrate that the aerosol loading was significantly high during the period of pollution

2 caused by wildfire haze.

3 **4.2 Chemical characteristics of wildfire haze particles**

4 Figures 3a-b show the time series of both the mass concentrations and the corresponding

5 mass fractions of organics, sulfate, nitrate, ammonium, and chloride (expressed as f_{org}, f_{SO4}^{2-},

6 f_{NO3}^{-}, f_{NH4}^{+}, and f_{Cl}^{-}, respectively) in NR-PM$_1$ quantified by the ToF-ACSM. The average mass

7 loading of NR-PM$_1$ was as high as 44.7 ± 24.5 µg m^{-3}, confirming the severity of the pervasive

8 wildfire haze. During the observation period, organics were always the most abundant

9 compounds in NR-PM$_1$ (34.8 ± 20.7 µg m^{-3}). The mass concentration of organics was higher

10 than 50.0 µg m^{-3} in many cases, and it occasionally exceeded 100.0 µg m^{-3}. On average,

11 organics accounted for the highest mass fraction of 77.1 %, followed by sulfate (11.7 %),

12 ammonium (6.4 %), and nitrate (4.2 %). The mass concentration of non-refractory chloride was

13 almost negligible (0.6 % of the total mass). These results demonstrate that the submicron wildfire

14 haze particles were predominantly composed of organics.

15 Table 2 summarizes the mass concentrations of all the analyzed inorganic ionic species in

16 the PM$_{2.5}$ filter samples. The corresponding data for carbonaceous fractions are presented in

17 Fig. 4. Overall, the mass fraction of EC varied from 4.4 % to 15.8 % with a mean value of

18 10.8 %. OC occupied 30.4−50.7 % of the total PM$_{2.5}$ mass concentration, and the mean fraction

19 was 43.0 %. The WSOC fraction was in the range of 17.6−30.2 % with the mean level of 26.7 %.

20 Correspondingly, the water-insoluble OC (WISOC) content was calculated to be 6.1−20.5 %

21 with the mean fraction of 16.3 %. The WSOC/OC ratios were consistently higher than 50.0 %

22 with a mean and maximum values of 63.6 % and 79.9 %, respectively. The mean WSOC/OC

23 value was significantly higher than that for fresh Indonesian peat burning particles emitted from

24 the source region (i.e., 16 %; Jayaranthe et al., 2017), which were demonstrated to be generally

25 water insoluble and thus nearly non-hygroscopic (Chen et al., 2017). This result suggests that the

26 majority of organics in the wildfire haze particles were water soluble, implying the importance of

27 secondary formation as well as the chemical transformation of organic particles during

28 atmospheric transport. Inorganic ions were less abundant and less variable than the organics were.

29 On average, the inorganics accounted for 30.5 % of the PM$_{2.5}$ mass loading with the mean

contributions of 0.6 % by Cl^-, 2.6 % by NO_3^-, 17.2 % by SO_4^{2-}, 0.4 % by Na^+, 8.1 % by NH_4^+, 0.8 % by K^+, 0.1 % by Mg^{2+}, and 0.7 % by Ca^{2+}. Sulfate, ammonium, and nitrate were the most abundant inorganic components. More than half of the inorganics was contributed by sulfate. These results show that the wildfire haze particles were dominated by organics especially water-soluble species. Mass concentrations of organics measured by the $PM_{2.5}$ filter samples and by the ToF-ACSM agreed well when the organics/OC ratio was assumed to be 1.4 (slope = 1.07; R^2 = 0.91) (Reid et al., 2005; Hallquist et al., 2009; Levin et al., 2010). The total mass concentrations of aerosol particles quantified by the filter samples and the ToF-ACSM also correlated well (R^2 = 0.96). The mass loading of the $PM_{2.5}$ filter samples was approximately 30 % higher than that of the ToF-ACSM results, likely because of the difference in particle size range and the lack of EC content for the ToF-ACSM measurements (Budisulistiorini et al., 2018).

Figure 3c shows the mean mass spectra of organics averaged over the observation period. Ion signals at m/z 43 (most likely $C_2H_3O^+$) and m/z 44 (CO_2^+) were prominent, accounting for 7.5 % and 10.5 % of the total organics mass spectrum. The predominant signal of m/z 44 indicates that organic compounds in wildfire haze particles were highly oxygenated. High-molecular weight organic signals with $m/z > 100$ possessed an abundance of 13.3 %. The marker ions for biomass burning particles, such as m/z 60 (mostly $C_2H_4O_2^+$) and m/z 73 (mainly $C_3H_5O_2^+$), which originating in levoglucosan-like species (e.g., levoglucosan, mannosan, and galactosan) were also clearly observed (Cubison et al., 2011).

Figures 6d-e show the mean contributions of four organic components classified by the ME-2 method, including HOA (8.8 % of NR-PM_1 mass), PBOA (10.4 %), BBOA (10.0 %), and OOA (36.0 %). The primary organics originating from biomass burning (i.e., PBOA and BBOA) accounted for 20.4 %. OOA was the dominant type of organics during the wildfire haze episodes.

4.3 Hygroscopic properties of wildfire haze particles

Figure 5 displays the time series of the mean *GF* data as well as the corresponding values of κ during the entire observation period. The mean values of *GF* varied between 0.98 and 1.52 with the average of 1.25 ± 0.09. *GF* values larger than 1.40 were normally observed in the afternoon. The variation in the corresponding κ results ranged from 0.004−0.475, and the average κ value was 0.189 ± 0.087. Table 3 summarizes the mean κ results for organics (cf.

Sect.3.2, with EC considered), which were calculated using the HTDMA and ToF-ACSM measurements during the overlapping observation period from 10−24 October 2015. The HTDMA-derived bulk κ results averaged over the same overlapping period were defined as κ_{HTDMA}. The mean κ_{org} (0.157 ± 0.108) was lower than the mean κ_{OOA} (0.266 ± 0.184), as the whole organic fraction normally contains both non-hygroscopic and hygroscopic organics. The derived κ_{org} results are demonstrated to be comparable to previously reported κ values for bulk organics (Petters and Kreidenweis, 2007; Duplissy et al., 2011; Lathem et al., 2013; Cerully et al., 2015). Moreover, the mean κ_{OOA} value agreed well with mean κ results in previous field and laboratory studies (e.g., κ = 0.25 ± 0.06 for biogenic OOA, Chang et al., 2010; κ = 0.2 ± 0.1 for aged BBOA, Engelhart et al., 2012). A caveat of this comparison is the representativeness of laboratory experiments for the actual environmental conditions, including types of burnt biomasses, concentrations and types of oxidants, and aging time. As the atmospheric condition of tropical Asia is unique, a systematic study of the chemical aging process of wildfire plume for the region would be required in the future. Note that the mean κ_{OOA} was even higher than the corresponding mean κ_{HTDMA} (0.207 ± 0.093), revealing that the water uptake particularly by some highly oxygenated organics in the wildfire haze particles could be highly significant.

4.4 Diurnal variations of hygroscopic properties and chemical composition

GF exhibited a clear pattern of diurnal variation (Fig. 6a). Higher GF values were observed during the daytime (GF = 1.27 ± 0.05 for 08:00−20:00 LT). However, the values were lower in the early morning and at night (1.23 ± 0.05 for 20:00−08:00 LT). The corresponding mean bulk κ results averaged over the entire observation period were 0.213 ± 0.051 for the daytime and 0.172 ± 0.043 for nighttime.

Similarly, the daytime mean κ_{org} and κ_{OOA} were 0.200 ± 0.104 and 0.323 ± 0.177, respectively, whereas the nighttime mean values were 0.103 ± 0.086 (κ_{org}) and 0.186 ± 0.177 (κ_{OOA}) (Table 3). These mean κ values were 19.2 % lower (κ_{org}) and 30.8 % higher (κ_{OOA}) than the concurrently measured mean κ_{HTDMA} result of 0.247 ± 0.096 (daytime), whereas they were 35.9 % lower (κ_{org}) and 16.3 % higher (κ_{OOA}) than that of 0.160 ± 0.063 (nighttime). A more significant discrepancy between κ_{org} and κ_{HTDMA} was observed at night, whereas a larger difference between κ_{OOA} and κ_{HTDMA} occurred during the day, which was likely due to the greatly

inhibited oxidation processes of organic compounds in the evening in contrast to the enhanced situations during the day. This correlation could be visually observed in the corresponding diurnal patterns of both mean *GF* and OA factors, as the fraction of OOA was demonstrated as a moderately good indicator of the hygroscopicity of organics (Ogawa et al., 2016).

The observed variation in *GF* was predominantly caused by diurnal variations in the probability distribution of *g* (Fig. 6b). Specifically, the number fractions of the highly hygroscopic mode particles were low in the early morning and evening ($nf_{highly} < 0.3$), and higher during the afternoon (approaching the highest level of 0.6 around 15:00 LT). The value was positively correlated with *GF* ($R = 0.97$). The number fraction of the weakly hygroscopic particles was opposite that of the highly hygroscopic particles, and it was negatively correlated with the mean *GF* ($R = -0.95$). There was no clear diurnal variation in the number fraction of the moderately hygroscopic mode particles (stable around 0.2). These results suggest that the water uptake by wildfire haze particles is closely related to the fractions of weakly and highly hygroscopic mode particles. The mean *g* values for each mode were 1.05 ± 0.02 for weakly, 1.21 ± 0.01 for moderately, and 1.40 ± 0.05 for highly hygroscopic particles. The average values for *nf* were 0.42 ± 0.18 for weakly, 0.18 ± 0.07 for moderately, and 0.40 ± 0.20 for highly hygroscopic particles (Table 4).

The diurnal variation in hygroscopic properties coincided with that in chemical compositions (Fig. 6c). The mean *GF* correlated well with f_{SO4}^{2-}, suggesting the primary role of f_{SO4}^{2-} in governing the water uptake by wildfire haze particles. The enhancement of f_{SO4}^{2-} accompanied decreased f_{org}. Variations in the chemical composition of organics also correlated well with the water uptake properties. The fraction of signal intensity at *m/z* 44 (f_{44}), which is considered as a marker ion for the degree of oxidation (Duplissy et al., 2011; Ng et al., 2011; Ogawa et al., 2016), was also high during the day, which was similar to the case of the mean *GF* and f_{SO4}^{2-}. A similar pattern was also observed in f_{OOA}, whereas that in HOA was the opposite (Fig. 6d). For instance, f_{HOA} was the highest during the morning rush hours, and it subsequently decreased throughout the day. Variations in the fresh PBOA fraction (f_{PBOA}) were similar to those of non-peat BBOA (f_{BBOA}) (Fig. 6e), namely, there was no apparent diurnal pattern during the severe wildfire haze periods. Consequently, the distinctly enhanced mean *GF* during the day could be attributed to the increase in both f_{SO4}^{2-} and f_{OOA}. Additionally, the local emission, which

1 primarily contributed to the HOA factor during morning/evening rush hours, could have

2 decreased the mean GF during these periods. The relative importance of both local emissions and

3 long-range transport might be influenced by meteorological conditions such as daily evolution of

4 planetary boundary layer (Krautstrunk et al., 2000; Geiß et al., 2017).

5 The diurnal variations in the organic composition were caused by the enhanced f_{OOA}

6 during the day, which accompanied decreases in f_{HOA}. In general, highly oxygenated organic

7 compounds are highly hygroscopic due to their water solubility, qualitatively explaining the

8 similarities in the diurnal variations among mean GF, f_{OOA}, and f_{44} (Duplissy et al., 2011; Zhao et

9 al., 2015; Ogawa et al., 2016). The relationship between the particle hygroscopicity and the

10 degree of oxidation of organics will be discussed in detail in Sect. 5.2.

5. Discussion

5.1 Chemical composition dependences of water uptake by wildfire haze particles

14 Figure 7 depicts the relationships between κ and the mass fractions of both inorganic and

15 organic species in NR-PM$_1$ in the data obtained during the day and at night. κ and f_{SO4}^{2-} were

16 positively correlated, demonstrating that sulfate was the most important compound in governing

17 water uptake by 100 nm wildfire haze particles due to its high hygroscopicity. Similarly, κ was

18 positively related to f_{NH4}^{+}, as it is the counter cation of sulfate. In contrast, κ was negatively

19 correlated with f_{org}, as organics are less hygroscopic than inorganic salts are. There was no clear

20 correlation between κ and f_{NO3}^{-}, implying that the small amount of nitrate had an insignificant

21 contribution to the variability in κ of wildfire haze particles. κ was almost independent of f_{Cl}^{-},

22 partially due to the limited availability of non-refractory chloride. These distinctly different

23 correlations between inorganics with mean κ likely reflect the different formation mechanisms of

24 these species. Sulfate formation occurs as a result of the photochemical process during the day,

25 whereas diurnal variations in gas–particle partitioning are important for the mass concentration

26 of nitrate or chloride (Aan de Brugh et al., 2012; Gong et al., 2013).

27 The correlation between κ and f_{org} was relatively scattered. For instance, κ varied from

28 0.10 to 0.40 when f_{org} was 0.7, signifying that factors other than f_{org} could influence the water

uptake. The variability in the chemical characteristics of organics might have played a role in the scattering of the data (Fig. 6d-f).

5.2 Relationship between the hygroscopicity and chemical composition of organics

Table 2 summarizes the κ_{org} and κ_{OOA} results averaged over the same PM$_{2.5}$ filter sampling periods. Figure 8 illustrates the relationship between κ_{org} and f_{WSOC}. In general, κ_{org} was insignificantly correlated with f_{WSOC}, especially in the data on October 22. The relatively high value of f_{44} (0.11) on October 22 might have caused the deviation. These results indicate that the oxygenation degree of organics could predominate over the WSOC fraction regarding the hygroscopic growth of organic-rich wildfire haze particles.

Figure 9 depicts the relationships between κ_{org} and f_{44} as well as κ_{org} and f_{44}/f_{43}. The daily average data were utilized. Although the data were scattered, a positive correlation between κ_{org} and f_{44} was observed ($R = 0.70$). The signal of m/z 44 (mostly CO_2^+) is known to originate in highly oxidized organic functional groups, such as dicarboxylic acids and acyl peroxides (Aiken et al., 2008). These highly oxygenated functional groups contribute to promoting hygroscopicity by enhancing water solubility (Topping et al., 2005; Cubison et al., 2006; Hallquist et al., 2009; Duplissy et al., 2011; Psichoudaki and Pandis, 2013; Suda et al., 2014; Riipinen et al., 2015; Ogawa et al., 2016; Petters et al., 2016; Marsh et al., 2017). κ_{org} and f_{44}/f_{43} also presented a similar trend to that of κ_{org} and f_{44}. The correlations shown in Figure 9 clearly demonstrate the important role of oxygenation degree in the water uptake properties of organic compounds in wildfire haze particles.

During the day, organic particles tend to be highly oxidized because of the oxidation of primary organic aerosol as well as the formation of secondary organic aerosol from volatile organic compounds (Ng et al., 2010 − see Fig. 6; Zhao et al., 2016). The chemical evolution processes of organic aerosol particles need to be better understood to enhance quantitative predictions of water uptake by wildfire haze particles (Kroll and Seinfeld, 2008; Riipinen et al., 2011; Winkler et al., 2012; Ehn et al., 2014). The evolution process could induce alternations in size dependence of chemical composition, and in the mixing state (Chakrabarty et al., 2006; Zhao et al., 2015). To address these unanswered questions, further knowledge about size- and

1 mixing state-dependent chemical composition as well as the molecular-level chemical

2 characteristics of Indonesian wildfire haze particles are required.

6. Conclusions

5 In September−October 2015, Indonesian wildfire-induced transboundary haze pollution

6 spread throughout Southeast Asia, affecting both environment and climate dramatically and

7 ravaging public health and the economy seriously. As a downwind receptor city, Singapore

8 experienced pervasive wildfire haze events. In this study, we simultaneously measured the

9 hygroscopic growth factor (*GF*) and the chemical composition of ambient wildfire haze particles

10 in Singapore, with the aim of providing comprehensive insights into the linkages between water

11 uptake and particle chemical composition as well as secondary aerosol formation.

12 High aerosol loading of non-refractory submicron particles (NR-PM$_1$, occasionally

13 exceeding 100.0 μg m^{-3}) was frequently observed, stressing the severity of the 2015 wildfire

14 haze pollution. The NR-PM$_1$ particles are predominantly composed of organics (OA,

15 approximately 77.1 % on average) and sulfate dominates the inorganic constituents (about

16 11.7 %). Chemical analyses of NR-PM$_1$ indicate the ubiquity and dominance of oxygenated

17 species in organics, in line with the most intense ion signals at *m/z* 44 (mostly CO_2^+, f_{44} = 10.5 %

18 in total OA mass) and *m/z* 43 (most likely $C_2H_3O^+$, f_{43} = 7.5 % on average). Moreover, a major

19 fraction of organics is water soluble, as signified by the high water-soluble organic carbon

20 fraction in ambient PM$_{2.5}$ filter samples (26.7 % of the total PM$_{2.5}$ mass).

21 Wildfire haze particles are generally highly hygroscopic. The hygroscopicity parameter, κ,

22 of 100 nm particles varied between 0.004 and 0.475, with a mean κ value of 0.189 ± 0.087. The

23 derived mean κ results of organics were 0.157 ± 0.108 (κ_{org}, bulk organics) and 0.266 ± 0.184

24 (κ_{OOA}, oxygenated organic fraction), which are comparable to previously reported values of

25 organic compounds (Petters and Kreidenweis, 2007; Duplissy et al., 2011; Lathem et al., 2013;

26 Cerully et al., 2015). These results highlight the difference in κ between wildfire haze particles

27 and fresh Indonesian peat burning particles, which are intrinsically non-hygroscopic due to the

28 rather limited water-soluble organic fraction (Chen et al., 2017). The *GF* data showed a notable

diurnal variation that usually peaked during the day. This variation was identical to the diurnal pattern of the number fraction of highly hygroscopic mode particles, and it accompanied the opposite fluctuation of the number fraction of weakly hygroscopic mode particles. These results imply the chemical composition dependence of particle hygroscopicity, as supported by the positive correlation of κ with the mass fraction of sulfate but its inverse relation to the mass fraction of organics. In addition to the governing influence of sulfate, κ of the haze particles was promoted by the water uptake of organics. Although κ_{org} was loosely related to the water-soluble organic fraction, a positive correlation between κ_{org} and f_{44} was shown ($R = 0.70$). This denotes that the oxygenation degree of organics may play an important role in water uptake especially by organic-rich haze particles.

To the best of our knowledge, this could be the first reported field measurements of water uptake by wildfire haze particles in Equatorial Asia. The results suggest that formation of secondary aerosol particles, including both inorganics and organics, is key in addressing the variability of reported results about the hygroscopic properties of aerosol particles originating from Indonesian peatland fires. Further quantitative studies on size-dependent chemical composition and detailed chemical analyses at molecular levels are needed to deepen our understanding of the water uptake by particles stemmed from Indonesian wildfires.

Acknowledgments

This work was supported by the Singapore National Research Foundation (NRF) under its Singapore National Research Fellowship scheme (National Research Fellow Award, NRF2012NRF-NRFF001-031), the NRF Campus for Research Excellence and Technological Enterprise (CREATE) program (NRF2016-ITCOO1-021), the Earth Observatory of Singapore, and Nanyang Technological University. Takuma Miyakawa and Yuichi Komazaki were funded by the Environment Research and Technology Development Fund (2-1403) of the Ministry of Environment, Japan and the Japan Society for the Promotion of Science (JSPS), KAKENHI Grant number JP26550021. We would like to thank Wen-Chien Lee and Gissella B. Lebron for assisting in the ambient haze observations. We also acknowledge the help of Pavel Adamek in revising our English.

1   **References**

2   Aan de Brugh, J. M. J., Henzing, J. S., Schaap, M., Morgan, W. T., van Heerwaarden, C. C.,
3   Weijers, E. P., Coe, H., and Krol, M. C.: Modelling the partitioning of ammonium nitrate in the
4   convective boundary layer, Atmos. Chem. Phys., 12, 3005-3023, 2012.

5   Aiken, A. C., DeCarlo, P. F., Kroll, J. H., Worsnop, D. R., Huffman, J. A., Docherty, K. S.,
6   Ulbrich, I. M., Mohr, C., Kimmel, J. R., Sueper, D., Sun, Y., Zhang, Q., Trimborn, A., Northway,
7   M., Ziemann, P. J., Canagaratna, M. R., Onasch, T. B., Alfarra, M. R., Prevot, A. S. H., Dommen,
8   J., Duplissy, J., Metzger, A., Baltensperger, U., and Jimenez, J. L.: O/C and OM/OC ratios of
9   primary, secondary, and ambient organic aerosols with high-resolution time-of-flight aerosol
10 mass spectrometry, Environ. Sci. Technol., 42, 4478-4485, 2008.

11 Allan, J. D., Jimenez, J. L., Williams, P. I., Alfarra, M. R., Bower, K. N., Jayne, J. T., Coe, H.,
12 and Worsnop, D. R.: Quantitative sampling using an Aerodyne aerosol mass spectrometer 1.
13 Techniques of data interpretation and error analysis, J. Geophys. Res. Atmos., 108, 4090,
14 doi:10.1029/2002JD002358, 2003.

15 Balasubramanian, R., Qian, W.-B., Decesari, S., Facchini, M. C., and Fuzzi, S.: Comprehensive
16 characterization of $PM_{2.5}$ aerosols in Singapore, J. Geophys. Res. Atmos., 108, 4523,
17 doi:10.1029/2002JD002517, 2003.

18 Bond, T. C. and Bergstrom, R. W.: Light absorption by carbonaceous particles: An investigative
19 review, Aerosol Sci. & Technol., 40, 27-67, 2006.

20 Bougiatioti, A., Bezantakos, S., Stavroulas, I., Kalivitis, N., Kokkalis, P., Biskos, G.,
21 Mihalopoulos, N., Papayannis, A., and Nenes, A.: Biomass-burning impact on CCN number,
22 hygroscopicity and cloud formation during summertime in the eastern Mediterranean, Atmos.
23 Chem. Phys., 16, 7389-7409, 2016.

24 Brechtel, F. J. and Kreidenweis, S. M.: Predicting particle critical supersaturation from
25 hygroscopic growth measurements in the humidified TDMA. Part II: laboratory and ambient
26 studies, J. Atmos. Sci., 57, 1872-1887, 2000.

27 Budisulistiorini S. H., Riva, M., Williams, M., Chen, J., Itoh, M., Surratt, J. D., and Kuwata, M.:
28 Light-absorbing brown carbon aerosol constituents from combustion of Indonesian peat and
29 biomass, Environ. Sci. & Technol., 51, 4415-4423, 2017.

30 Budisulistiorini, S. H., Riva, M., Williams, M., Miyakawa, T., Chen, J., Itoh, M., Surratt, J. D.,
31 and Kuwata, M.: Dominant contribution of oxygenated organic aerosol to haze particles from
32 real-time observation in Singapore during an Indonesian wildfire event in 2015. Atmos. Chem.
33 Phys. Discuss., https://doi.org/10.5194/acp-2018-217, in review, 2018.

34 Canonaco, F., Crippa, M., Slowik, J. G., Baltensperger, U., and Prévôt, A. S. H.: SoFi, an IGOR-
35 based interface for the efficient use of the generalized multilinear engine (ME-2) for the source
36 apportionment: ME-2 application to aerosol mass spectrometer data, Atmos. Meas. Tech., 6,
37 3649-3661, 2013.

38 Carrico, C. M., Petters, M. D., Kreidenweis, S. M., Collett Jr., J. L., Engling, G., and Malm, W.
39 C.: Aerosol hygroscopicity and cloud droplet activation of extracts of filters from biomass
40 burning experiments, J. Geophys. Res. Atmos., 113, D08206, doi:10.1029/2007JD009274, 2008.

Carrico, C. M., Petters, M. D., Kreidenweis, S. M., Sullivan, A. P., McMeeking, G. R., Levin, E. J. T., Engling, G., Malm, W. C., and Collett Jr., J. L.: Water uptake and chemical composition of fresh aerosols generated in open burning of biomass, Atmos. Chem. Phys., 10, 5165-5178, 2010.

Cerully, K. M., Bougiatioti, A., Hite Jr, J. R., Guo, H., Xu, L., Ng, N. L., Weber, R., and Nenes, A.: On the link between hygroscopicity, volatility, and oxidation state of ambient and water-soluble aerosols in the southeastern United States, Atmos. Chem. Phys., 15, 8679-8694, 2015.

Chakrabarty, R. K., Moosmuller, H., Garro, M. A., Arnott, W. P., Walker, J., Susott, R. A., Babbitt, R. E., Wold, C. E., Lincoln, E. N., and Hao, W. M.: Emissions from the laboratory combustion of wildland fuels: Particle morphology and size, J. Geophys. Res., 111, D07204, doi:10.1029/2005JD006659, 2006.

Chan, M. N. and Chan, C. K.: Hygroscopic properties of two model humic-like substances and their mixtures with inorganics of atmospheric importance, Environ. Sci. & Technol., 37, 5109-5115, 2003.

Chan, M. N., Choi, M. Y., Ng, N. L., and Chan, C. K.: Hygroscopicity of water-soluble organic compounds in atmospheric aerosols: Amino acids and biomass burning derived organic species, Environ. Sci. & Technol., 39, 1555-1562, 2005.

Chand, D., Schmid, O., Gwaze, P., Parmar, R. S., Helas, G., Zeromskiene, K., Wiedensohler, A., Massling, A., and Andreae, M. O.: Laboratory measurements of smoke optical properties from the burning of Indonesian peat and other types of biomass, Geophys. Res. Lett., 32, L12819, doi:10.1029/2005GL022678, 2005.

Chang, R. Y. W., Slowik, J. G., Shantz, N. C., Vlasenko, A., Liggio, J., Sjostedt, S. J., Leaitch, W. R., and Abbatt, J. P. D.: The hygroscopicity parameter (κ) of ambient organic aerosol at a field site subject to biogenic and anthropogenic influences: relationship to degree of aerosol oxidation, Atmos. Chem. Phys., 10, 5047-5064, 2010.

Chen, J., Budisulistiorini, S. H., Itoh, M., Lee, W.-C., Miyakawa, T., Komazaki, Y., Yang, L., and Kuwata, M.: Water uptake by fresh Indonesian peat burning particles is limited by water soluble organic matter, Atmos. Chem. Phys., 17, 11591-11604, 2017.

Chow, J. C., Watson, J. G., Pritchett, L. C., Pierson, W. R., Frazier, C. A., and Purcell, R. G.: The DRI thermal/optical reflectance carbon analysis system: Description, evaluation and applications in U.S. air quality studies, Atmos. Environ., 27A, 1185-1201, 1993.

Crippa, P., Castruccio, S., Archer-Nicholls, S., Lebron, G. B., Kuwata, M., Thota, A., Sumin, S., Butt, E., Wiedinmyer, C., and Spracklen, D. V.: Population exposure to hazardous air quality due to the 2015 fires in Equatorial Asia, Sci. Rep., 6, 37074, doi:10.1038/srep37074, 2016.

Cross, E. S., Slowik, J. G., Davidovits, P., Allan, J. D., Worsnop, D. R., Jayne, J. T., Lewis, D. K., Canagaratna, M., and Onasch, T. B.: Laboratory and ambient particle density determinations using light scattering in conjunction with aerosol mass spectrometry, Aerosol Sci. Technol., 41, 343-359, 2007.

Cubison, M. J., Alfarra, M. R., Allan, J., Bower, K. N., Coe, H., McFiggans, G. B., Whitehead, J. D., Williams, P. I., Zhang, Q., Jimenez, J. L., Hopkins, J., and Lee, J.: The characterisation of pollution aerosol in a changing photochemical environment, Atmos. Chem. Phys., 6, 5573-5588, 2006.

Cubison, M. J., Ortega, A. M., Hayes, P. L., Farmer, D. K., Day, D., Lechner, M. J., Brune, W. H., Apel, E., Diskin, G. S., Fisher, J. A., Fuelberg, H. E., Hecobian, A., Knapp, D. J., Mikoviny, T., Riemer, D., Sachse, G. W., Sessions, W., Weber, R. J., Weinheimer, A. J., Wisthaler, A., and Jimenez, J. L.: Effects of aging on organic aerosol from open biomass burning smoke in aircraft and laboratory studies, Atmos. Chem. Phys., 11, 12049-12064, 2011.

Dick, W. D., Saxena, P., and McMurry, P. H.: Estimation of water uptake by organic compounds in submicron aerosols measured during the Southeastern Aerosol and Visibility Study, J. Geophys. Res. Atmos., 105, 1471-1479, 2000.

Dinar, E., Taraniuk, I., Graber, E. R., Anttila, T., Mentel, T. F., and Rudich, Y.: Hygroscopic growth of atmospheric and model humic-like substances, J. Geophys. Res., 112, D05211, doi:10.1029/2006JD007442, 2007.

Duncan, B. N., Bey, I., Chin, M., Mickley, L. J., Fairlie, T. D., Martin, R. V., and Matsueda, H.: Indonesian wildfires of 1997: Impact on tropospheric chemistry, J. Geophys. Res. Atmos., 108, 4458, doi:10.1029/2002JD003195, 2003.

Duplissy, J., DeCarlo, P. F., Dommen, J., Alfarra, M. R., Metzger, A., Barmpadimos, I., Prevot, A. S. H., Weingartner, E., Tritscher, T., Gysel, M., Aiken, A. C., Jimenez, J. L., Canagaratna, M. R., Worsnop, D. R., Collins, D. R., Tomlinson, J., and Baltensperger, U.: Relating hygroscopicity and composition of organic aerosol particulate matter, Atmos. Chem. Phys., 11, 1155-1165, 2011.

Duplissy, J., Gysel, M., Alfarra, M. R., Dommen, J., Metzger, A., Prévôt, A. S. H., Weingartner, E., Laaksonen, A., Raatikainen, T., Good, N., Turner, S. F., McFiggans, G., and Baltensperger, U.: Cloud forming potential of secondary organic aerosol under near atmospheric conditions, Geophys. Res. Lett., 35, L03818, doi:10.1029/2007GL031075, 2008.

Duplissy, J., Gysel, M., Sjogren, S., Meyer, N., Good, N., Kammermann, L., Michaud, V., Weigel, R., Martins dos Santos, S., Gruening, C., Villani, P., Laj, P., Sellegri, K., Metzger, A., McFiggans, G. B., Wehrle, G., Richter, R., Dommen, J., Ristovski, Z., Baltensperger, U., and Weingartner, E.: Intercomparison study of six HTDMAs: results and recommendations, Atmos. Meas. Tech., 2, 363-378, 2009.

Dusek, U., Frank, G. P., Helas, G., Iinuma, Y., Zeromskiene, K., Gwaze, P., Hennig, T., Massling, A., Schmid, O., Herrmann, H., Wiedensohler, A., and Andreae, M. O.: "Missing" cloud condensation nuclei in peat smoke, Geophys. Res. Lett., 32, L11802, doi:10.1029/2005GL022473, 2005.

Ehn, M., Thornton, J. A., Kleist, E., Sipila, M., Junninen, H., Pullinen, I., Springer, M., Rubach, F., Tillmann, R., Lee, B., Lopez-Hilfiker, F., Andres, S., Acir, I.-H., Rissanen, M., Jokinen, T., Schobesberger, S., Kangasluoma, J., Kontkanen, J., Nieminen, T., Kurten, T., Nielsen, L. B., Jorgensen, S., Kjaergaard, H. G., Canagaratna, M., Maso, M. D., Berndt, T., Petaja, T., Wahner, A., Kerminen, V.-M., Kulmala, M., Worsnop, D. R., Wildt, J., and Mentel, T. F.: A large source of low-volatility secondary organic aerosol, Nature, 506, 476-479, 2014.

Engelhart, G. J., Hennigan, C. J., Miracolo, M. A., Robinson, A. L., and Pandis, S. N.: Cloud condensation nuclei activity of fresh primary and aged biomass burning aerosol, Atmos. Chem. Phys., 12, 7285-7293, 2012.

Field, R. D., van der Werf, G. R., Fanin, T., Fetzer, E. J., Fuller, R., Jethva, H., Levy, R., Livesey, N. J., Luo, M., Torres, O., and Worden, H. M.: Indonesian fire activity and smoke pollution in 2015 show persistent nonlinear sensitivity to El Niño-induced drought, Proc. Natl. Acad. Sci., 113, 9204-9209, 2016.

Fröhlich, R., Cubison, M. J., Slowik, J. G., Bukowiecki, N., Prévôt, A. S. H., Baltensperger, U., Schneider, J., Kimmel, J. R., Gonin, M., Rohner, U., Worsnop, D. R., and Jayne, J. T.: The ToF-ACSM: a portable aerosol chemical speciation monitor with TOFMS detection, Atmos. Meas. Tech., 6, 3225-3241, 2013.

Geiß, A., Wiegner, M., Bonn, B., Schäfer, K., Forkel, R., von Schneidemesser, E., Münkel, C., Chan, K. L., and Nothard, R.: Mixing layer height as an indicator for urban air quality?, Atmos. Meas. Tech., 10, 2969-2988, 2017.

Gong, L., Lewicki, R., Griffin, R. J., Tittel, F. K., Lonsdale, C. R., Stevens, R. G., Pierce, J. R., Malloy, Q. G. J., Travis, S. A., Bobmanuel, L. M., Lefer, B. L., and Flynn, J. H.: Role of atmospheric ammonia in particulate matter formation in Houston during summertime, Atmos. Environ., 77, 893-900, 2013.

Gras, J. L., Jensen, J. B., Okada, K., Ikegami, M., Zaizen, Y., and Makino, Y.: Some optical properties of smoke aerosol in Indonesia and tropical Australia, Geophys. Res. Lett., 26, 1393-1396, 1999.

Gunthe, S. S., King, S. M., Rose, D., Chen, Q., Roldin, P., Farmer, D. K., Jimenez, J. L., Artaxo, P., Andreae, M. O., Martin, S. T., and Pöschl, U.: Cloud condensation nuclei in pristine tropical rainforest air of Amazonia: size-resolved measurements and modeling of atmospheric aerosol composition and CCN activity, Atmos. Chem. Phys., 9, 7551-7575, 2009.

Gysel, M., Crosier, J., Topping, D. O., Whitehead, J. D., Bower, K. N., Cubison, M. J., Williams, P. I., Flynn, M. J., McFiggans, G. B., and Coe, H.: Closure study between chemical composition and hygroscopic growth of aerosol particles during TORCH2, Atmos. Chem. Phys., 7, 6131-6144, 2007.

Gysel, M., McFiggans, G. B., and Coe, H.: Inversion of tandem differential mobility analyser (TDMA) measurements, J. Aerosol Sci., 40, 134-151, 2009.

Gysel, M., Weingartner, E., Nyeki, S., Paulsen, D., Baltensperger, U., Galambos, I., and Kiss, G.: Hygroscopic properties of water-soluble matter and humic-like organics in atmospheric fine aerosol, Atmos. Chem. Phys., 4, 35-50, 2004.

Hallar, A. G., Lowenthal, D. H., Clegg, S. L., Samburova, V., Taylor, N., Mazzoleni, L. R., Zielinska, B. K., Kristensen, T. B., Chirokova, G., McCubbin, I. B., Dodson, C., and Collins, D.: Chemical and hygroscopic properties of aerosol organics at Storm Peak Laboratory, J. Geophys. Res. Atmos., 118, 4767-4779, 2013.

Hallquist, M., Wenger, J. C., Baltensperger, U., Rudich, Y., Simpson, D., Claeys, M., Dommen, J., Donahue, N. M., George, C., Goldstein, A. H., Hamilton, J. F., Herrmann, H., Hoffmann, T., Iinuma, Y., Jang, M., Jenkin, M. E., Jimenez, J. L., Kiendler-Scharr, A., Maenhaut, W., McFiggans, G., Mentel, Th. F., Monod, A., Prévôt, A. S. H., Seinfeld, J. H., Surratt, J. D., Szmigielski, R., and Wildt, J.: The formation, properties and impact of secondary organic aerosol: current and emerging issues, Atmos. Chem. Phys., 9, 5155-5236, 2009.

Huijnen, V., Wooster, M. J., Kaiser, J. W., Gaveau, D. L. A., Flemming, J., Parrington, M., Inness, A., Murdiyarso, D., Main, B., and van Weele, M.: Fire carbon emissions over maritime southeast Asia in 2015 largest since 1997, Sci. Rep., 6, 26886, doi:10.1038/srep26886, 2016.

Jayarathne, T., Stockwell, C. E., Gilbert, A. A., Daugherty, K., Cochrane, M. A., Ryan, K. C., Putra, E. I., Saharjo, B. H., Nurhayati, A. D., Albar, I., Yokelson, R. J., and Stone, E. A.: Chemical characterization of fine particulate matter emitted by peat fires in Central Kalimantan, Indonesia, during the 2015 El Niño, Atmos. Chem. Phys., 18, 2585–2600, 2018.

Jimenez, J. L., Canagaratna, M. R., Donahue, N. M., Prevot, A. S. H., Zhang, Q., Kroll, J. H., DeCarlo, P. F., Allan, J. D., Coe, H., Ng, N. L., Aiken, A. C., Docherty, K. S., Ulbrich, I. M., Grieshop, A. P., Robinson, A. L., Duplissy, J., Smith, J. D., Wilson, K. R., Lanz, V. A., Hueglin, C., Sun, Y. L., Tian, J., Laaksonen, A., Raatikainen, T., Rautiainen, J., Vaattovaara, P., Ehn, M., Kulmala, M., Tomlinson, J. M., Collins, D. R., Cubison, M. J., Dunlea, J., Huffman, J. A., Onasch, T. B., Alfarra, M. R., Williams, P. I., Bower, K., Kondo, Y., Schneider, J., Drewnick, F., Borrmann, S., Weimer, S., Demerjian, K., Salcedo, D., Cottrell, L., Griffin, R., Takami, A., Miyoshi, T., Hatakeyama, S., Shimono, A., Sun, J. Y, Zhang, Y. M., Dzepina, K., Kimmel, J. R., Sueper, D., Jayne, J. T., Herndon, S. C., Trimborn, A. M., Williams, L. R., Wood, E. C., Middlebrook, A. M., Kolb, C. E., Baltensperger, U., and Worsnop, D. R.: Evolution of organic aerosols in the atmosphere, Science, 326, 1525-1529, 2009.

Johnston, F. H., Henderson, S.B., Chen, Y., Randerson, J. T., Marlier, M., DeFries, R. S., Kinney, P., Bowman, D. M., and Brauer, M.: Estimated global mortality attributable to smoke from landscape fires, Environ. Health Perspect., 120, 695-701, 2012.

Keywood, M. D., Ayers, G. P., Gras, J. L., Boers, R., and Leong, C. P.: Haze in the Klang Valley of Malaysia, Atmos. Chem. Phys., 3, 591-605, 2003.

King, S. M., Rosenoern, T., Shilling, J. E., Chen, Q., and Martin, S. T.: Cloud condensation nucleus activity of secondary organic aerosol particles mixed with sulfate, Geophys. Res. Lett., 34, L24806, doi:10.1029/2007GL030390, 2007.

Konecny, K., Ballhorn, U., Navratil, P., Jubanski, J., Page, S. E., Tansey, K., Hooijer, A., Vernimmen, R., and Siegert, F.: Variable carbon losses from recurrent fires in drained tropical peatlands, Glob. Change Biol., 22, 1469-1480, 2016.

Koplitz, S. N., Mickley, L. J., Marlier, M. E., Buonocore, J. J., Kim, P. S., Liu, T., Sulprizio, M. P., DeFries, R. S., Jacob, D. J., Schwartz, J., Pongsiri, M., and Myers, S. S.: Public health impacts of the severe haze in Equatorial Asia in September–October 2015: demonstration of a new framework for informing fire management strategies to reduce downwind smoke exposure, Environ. Res. Lett., 11, 094023, doi:10.1088/1748-9326/11/9/094023, 2016.

Krautstrunk, M., Neumann-Hauf, G., Schlager, H., Klemm, O., Beyrich, F., Corsmeier, U., Kalthoff, N., and Kotzian, M.: An experimental study on the planetary boundary layer transport of air pollutants over East Germany. Atmos. Environ., 34, 1247-1266, 2000.

Kreidenweis, S. M., Petters, M. D., and DeMott, P. J.: Single-parameter estimates of aerosol water content, Environ. Res. Lett., 3, 035002, doi:10.1088/1748-9326/3/3/035002, 2008.

Kristensen, T. B., Wex, H., Nekat, B., Nøjgaard, J. K., van Pinxteren, D., Lowenthal, D. H., Mazzoleni, L. R., Dieckmann, K., Bender Koch, C., Mentel, T. F., Herrmann, H., Hallar, A. G.,

Stratmann, F., and Bilde, M.: Hygroscopic growth and CCN activity of HULIS from different environments, J. Geophys. Res. Atmos., 117, D22203, doi:10.1029/2012JD018249, 2012.

Kroll, J. H. and Seinfeld, J. H.: Chemistry of secondary organic aerosol: Formation and evolution of low-volatility organics in the atmosphere, Atmos. Environ., 42, 3593-3624, 2008.

Kunii, O., Kanagawa, S., Yajima, I., Hisamatsu, Y., Yamamura, S., Amagai, T., and Ismail, Ir T. S.: The 1997 haze disaster in Indonesia: Its air quality and health effects, Archives of Environmental Health: An International Journal, 57, 16-22, 2002.

Kuwata, M., Zorn, S. R., and Martin, S. T.: Using elemental ratios to predict the density of organic material composed of carbon, hydrogen, and oxygen, Environ. Sci. & Technol., 46, 787-794, 2012.

Langner A, Miettinen J, and Siegert F.: Land cover change 2002–2005 in Borneo and the role of fire derived from MODIS imagery, Glob. Change Biol., 13, 2329-2340, 2007.

Lanz, V. A., Alfarra, M. R., Baltensperger, U., Buchmann, B., Hueglin, C., and Prévôt, A. S. H.: Source apportionment of submicron organic aerosols at an urban site by factor analytical modelling of aerosol mass spectra, Atmos. Chem. Phys., 7, 1503-1522, 2007.

Lathem, T. L., Beyersdorf, A. J., Thornhill, K. L., Winstead, E. L., Cubison, M. J., Hecobian, A., Jimenez, J. L., Weber, R. J., Anderson, B. E., and Nenes, A.: Analysis of CCN activity of Arctic aerosol and Canadian biomass burning during summer 2008, Atmos. Chem. Phys., 13, 2735-2756, 2013.

Lelieveld, J., Evans, J. S., Fnais, M., Giannadaki, D., and Pozzer, A.: The contribution of outdoor air pollution sources to premature mortality on a global scale, Nature, 525, 367-371, 2015.

Levin, E. J. T., McMeeking, G. R., Carrico, C. M., Mack, L., Kreidenweis, S. M., Wold, C. E., Moosmueller, H., Arnott, W. P., Hao, W. M., Collett, J. L., and Malm, W. C.: Biomass burning smoke aerosol properties measured during FLAME 2, J. Geophys. Res., 115, D18210, doi:10.1029/2009JD013601, 2010.

Lin, N.-H., Tsay, S.-C., Maring, H. B., Yen, M.-C., Sheu, G.-R., Wang, S.-H., Chi, K. H., Chuang, M.-T., Ou-Yang, C.-F., Fu, J. S., Reid, J. S., Lee, C.-T., Wang, L.-C., Wang, J.-L., Hsu, C. N., Sayer, A. M., Holben, B. N., Chu, Y.-C., Nguyen, X. A., Sopajaree, K., Chen, S.-J., Cheng, M.-T., Tsuang, B.-J., Tsai, C.-J., Peng, C.-M., Schnell, R. C., Conway, T., Chang, C.-T., Lin, K.-S., Tsai, Y. I., Lee, W.-J., Chang, S.-C., Liu, J.-J., Chiang, W.-L., Huang, S.-J., Lin, T.-H., and Liu, G.-R.: An overview of regional experiments on biomass burning aerosols and related pollutants in Southeast Asia: From BASE-ASIA and the Dongsha Experiment to 7-SEAS, Atmos. Environ., 78, 1-19, 2013.

Marcolli C., Luo B., and Peter, T.: Mixing of the organic aerosol fractions: liquids as the thermodynamically stable phases, J. Phys. Chem. A, 108, 2216-2224, 2004.

Marlier, M. E., DeFries, R., Pennington, D., Nelson, E., Ordway, E. M., Lewis, J., Koplitz, S. N., and Mickley, L. J.: Future fire emissions associated with projected land use change in Sumatra, Glob. Change Biol., 21, 345-362, 2015.

Marlier, M. E., DeFries, R. S., Voulgarakis, A., Kinney, P. L., Randerson, J. T., Shindell, D. T., Chen, Y., and Faluvegi, G.: El Niño and health risks from landscape fire emissions in southeast Asia, Nat. Clim. Change, 3, 131-136, 2013.

Marsh, A., Miles, R. E. H., Rovelli, G., Cowling, A. G., Nandy, L., Dutcher, C. S., and Reid, J. P.: Influence of organic compound functionality on aerosol hygroscopicity: Dicarboxylic acids, alkyl-substituents, sugars and amino acids, Atmos. Chem. Phys., 17, 5583-5599, 2017.

Massling, A., Leinert, S., Wiedensohler, A., and Covert, D.: Hygroscopic growth of sub-micrometer and one-micrometer aerosol particles measured during ACE-Asia, Atmos. Chem. Phys., 7, 3249-3259, 2007.

Massling, A., Wiedensohler, A., Busch, B., Neusüß, C., Quinn, P., Bates, T., and Covert, D.: Hygroscopic properties of different aerosol types over the Atlantic and Indian Oceans, Atmos. Chem. Phys., 3, 1377-1397, 2003.

Massoli, P., Lambe, A. T., Ahern, A. T., Williams, L. R., Ehn, M., Mikkilä, J., Canagaratna, M. R., Brune, W. H., Onasch, T. B., Jayne, J. T., Petäjä, T., Kulmala, M., Laaksonen, A., Kolb, C. E., Davidovits, P., and Worsnop, D. R.: Relationship between aerosol oxidation level and hygroscopic properties of laboratory generated secondary organic aerosol (SOA) particles, Geophys. Res. Lett., 37, L24801, doi:10.1029/2010GL045258, 2010.

Mircea, M., Facchini, M. C., Decesari, S., Cavalli, F., Emblico, L., Fuzzi, S., Vestin, A., Rissler, J., Swietlicki, E., Frank, G., Andreae, M. O., Maenhaut, W., Rudich, Y., and Artaxo, P.: Importance of the organic aerosol fraction for modeling aerosol hygroscopic growth and activation: a case study in the Amazon Basin, Atmos. Chem. Phys., 5, 3111-3126, 2005.

Ng, N. L., Canagaratna, M. R., Jimenez, J. L., Chhabra, P. S., Seinfeld, J. H., and Worsnop, D. R.: Changes in organic aerosol composition with aging inferred from aerosol mass spectra, Atmos. Chem. Phys., 11, 6465-6474, 2011.

Ng, N. L., Canagaratna, M. R., Zhang, Q., Jimenez, J. L., Tian, J., Ulbrich, I. M., Kroll, J. H., Docherty, K. S., Chhabra, P. S., Bahreini, R., Murphy, S. M., Seinfeld, J. H., Hildebrandt, L., Donahue, N. M., DeCarlo, P. F., Lanz, V. A., Prevot, A. S. H., Dinar, E., Rudich, Y., and Worsnop, D. R.: Organic aerosol components observed in northern hemispheric datasets from aerosol mass spectrometry, Atmos. Chem. Phys., 10, 4625-4641, 2010.

Ogawa, S., Setoguchi, Y., Kawana, K., Nakayama, T., Ikeda, Y., Sawada, Y., Matsumi, Y., and Mochida, M.: Hygroscopicity of aerosol particles and CCN activity of nearly hydrophobic particles in the urban atmosphere over Japan during summer, J. Geophys. Res. Atmos., 121, 7215-7234, 2016.

Paatero, P. and Tapper, U.: Positive matrix factorization: A nonnegative factor model with optimal utilization of error estimates of data values, Environmetrics, 5, 111-126, 1994.

Page, S. E., Siegert, F., Rieley, J. O., Boehm, H.-D. V., Jaya, A., and Limin, S.: The amount of carbon released from peat and forest fires in Indonesia during 1997, Nature, 420, 61-65, 2002.

Page, S., Hoscilo, A., Langner, A., Tansey, K., Siegert, F., Limin, S., and Rieley, J.: Tropical peatland fires in Southeast Asia, in: Tropical Fire Ecology: Climate Change, Land Use and Ecosystem Dynamics, Cochrane, M. A. (Ed.), Springer-Praxis, Heidelberg, Germany, 645, 2009.

Park, K., Kittelson, D. B., Zachariah, M. R., and McMurry, P. H.: Measurement of inherent material density of nanoparticle agglomerates, J. Nanopart. Res., 6, 267-272, 2004.

Peng, C., Chan, M. N., and Chan, C. K.: The hygroscopic properties of dicarboxylic and multifunctional acids: Measurements and UNIFAC predictions, Environ. Sci. Technol, 35, 4495-4501, 2001.

Petters, M. D., Carrico, C. M., Kreidenweis, S. M., Prenni, A. J., DeMott, P. J., Collett Jr., J. L., and Moosmuller, H.: Cloud condensation nucleation activity of biomass burning aerosol, J. Geophys. Res. Atmos., 114, D22205, doi:10.1029/2009JD012353, 2009.

Petters, M. D. and Kreidenweis, S. M.: A single parameter representation of hygroscopic growth and cloud condensation nucleus activity, Atmos. Chem. Phys., 7, 1961-1971, 2007.

Petters, M. D., Kreidenweis, S. M., and Ziemann, P. J.: Prediction of cloud condensation nuclei activity for organic compounds using functional group contribution methods, Geosci. Model Dev., 9, 111-124, 2016.

Psichoudaki, M. and Pandis, S. N.: Atmospheric aerosol water-soluble organic carbon measurement: A theoretical analysis, Environ. Sci. & Technol., 47, 9791-9798, 2013.

Reid, J. S., Hyer, E. J., Johnson, R. S., Holben, B. N., Yokelson, R. J., Zhang, J., Campbell, J. R., Christopher, S. A., Girolamo, L. D., Giglio, L., Holz, R. E., Kearney, C., Miettinen, J., Reid, E. A., Turk, F. J., Wang, J., Xian, P., Zhao, G., Balasubramanian, R., Chew, B. N., Janjai, S., Lagrosas, N., Lestari, P., Lin, N.-H., Mahmud, M., Nguyen, A. X., Norris, B., Oanh, N. T. K., Oo, M., Salinas, S. V., Welton, E. J., and Liew, S. C.: Observing and understanding the Southeast Asian aerosol system by remote sensing: An initial review and analysis for the Seven Southeast Asian Studies (7SEAS) program, Atmos. Res., 122, 403-468, 2013.

Reid, J. S., Koppmann, R., Eck, T. F., and Eleuterio, D. P.: A review of biomass burning emissions part II: intensive physical properties of biomass burning particles, Atmos. Chem. Phys., 5, 799-825, 2005.

Riipinen, I., Pierce, J. R., Yli-Juuti, T., Nieminen, T., Häkkinen, S., Ehn, M., Junninen, H., Lehtipalo, K., Petäjä, T., Slowik, J., Chang, R., Shantz, N. C., Abbatt, J., Leaitch, W. R., Kerminen, V. M., Worsnop, D. R., Pandis, S. N., Donahue, N. M., and Kulmala, M.: Organic condensation: a vital link connecting aerosol formation to cloud condensation nuclei (CCN) concentrations, Atmos. Chem. Phys., 11, 3865-3878, 2011.

Riipinen, I., Rastak, N., and Pandis, S. N.: Connecting the solubility and CCN activation of complex organic aerosols: a theoretical study using solubility distributions, Atmos. Chem. Phys., 15, 6305-6322, 2015.

Robinson, A. L., Donahue, N. M., Shrivastava, M. K., Weitkamp, E. A., Sage, A. M., Grieshop, A. P., Lane, T. E., Pierce, J. R., and Pandis, S. N.: Rethinking organic aerosols: Semivolatile emissions and photochemical aging, Science, 315, 1259-1262, 2007.

Rose, D., Nowak, A., Achtert, P., Wiedensohler, A., Hu, M., Shao, M., Zhang, Y., Andreae, M. O., and Pöschl, U.: Cloud condensation nuclei in polluted air and biomass burning smoke near the mega-city Guangzhou, China – Part 1: Size-resolved measurements and implications for the modeling of aerosol particle hygroscopicity and CCN activity, Atmos. Chem. Phys., 10, 3365-3383, 2010.

Rosenfeld, D.: TRMM observed first direct evidence of smoke from forest fires inhibiting rainfall, Geophys. Res. Lett., 26, 3105-3108, 1999.

Saxena, E, Hildemann, L. M., McMurry, E H., and Seinfeld, J. H.: Organics alter hygroscopic behavior of atmospheric particles, J. Geophys. Res., 100, 18755-18770, 1995.

See, S. W., Balasubramanian, R., and Wang, W.: A study of the physical, chemical, and optical properties of ambient aerosol particles in Southeast Asia during hazy and nonhazy days, J. Geophys. Res. Atmos., 111, D10S08, doi:10.1029/2005JD006180, 2006.

Spracklen, D. V., Reddington, C. L., and Gaveau, D. L. A.: Industrial concessions, fires and air pollution in Equatorial Asia, Environ. Res. Lett., 10, 091001, doi:10.1088/1748-9326/10/9/091001, 2015.

Stockwell, C. E., Jayarathne, T., Cochrane, M. A., Ryan, K. C., Putra, E. I., Saharjo, B. H., Nurhayati, A. D., Albar, I., Blake, D. R., Simpson, I. J., Stone, E. A., and Yokelson, R. J.: Field measurements of trace gases and aerosols emitted by peat fires in Central Kalimantan, Indonesia, during the 2015 El Niño, Atmos. Chem. Phys., 16, 11711-11732, 2016.

Stokes, R. H. and Robinson, R. A.: Interactions in aqueous nonelectrolyte solutions: I. Solute-solvent equilibria, J. Phys. Chem., 70, 2126-2130, 1966.

Suda, S. R., Petters, M. D., Yeh, G. K., Strollo, C., Matsunaga, A., Faulhaber, A., Ziemann, P. J., Prenni, A. J., Carrico, C. M., Sullivan, R. C., and Kreidenweis, S. M.: Influence of functional groups on organic aerosol cloud condensation nucleus activity, Environ. Sci. & Technol., 48, 10182-10190, 2014.

Topping, D. O., McFiggans, G. B., and Coe, H.: A curved multicomponent aerosol hygroscopicity model framework: Part 2 - Including organic compounds, Atmos. Chem. Phys., 5, 1223-1242, 2005.

Turpin, B. J., Hering, S. V., and Huntzicker, J. J.: Investigation of organic aerosol sampling artifacts in the Los Angeles Basin, Atmos. Environ., 28, 3061-3071, 1994.

Ulbrich, I. M., Canagaratna, M. R., Zhang, Q., Worsnop, D. R., and Jimenez, J. L.: Interpretation of organic components from positive matrix factorization of aerosol mass spectrometric data, Atmos. Chem. Phys., 9, 2891-2918, 2009.

van der Werf, G.R., Randerson, J. T., Giglio, L., Collatz, G. J., Mu, M., Kasibhatla, P. S., Morton, D. C., DeFries, R. S., Jin, Y., and van Leeuwen, T. T.: Global fire emissions and the contribution of deforestation, savanna, forest, agricultural, and peat fires (1997−2009), Atmos. Chem. Phys., 10, 11707-11735, 2010.

Whitehead, J. D., Darbyshire, E.,Brito, J., Barbosa, H. M. J., Crawford, I., Stern, R., Gallagher, M. W., Kaye, P. H., Allan, J. D., Coe, H., Artaxo, P., and McFiggans, G.: Biogenic cloud nuclei in the central Amazon during the transition from wet to dry season. Atmos. Chem. Phys., 16, 9727-9743, 2016.

Whitehead, J. D., Irwin, M., Allan, J. D., Good, N., and McFiggans, G.: A meta-analysis of particle water uptake reconciliation studies. Atmos. Chem. Phys., 14, 11833-11841, 2014.

Winkler, P. M., Ortega, J., Karl, T., Cappellin, L., Friedli, H. R., Barsanti, K., McMurry, P. H., and Smith, J. N.: Identification of the biogenic compounds responsible for size-dependent nanoparticle growth, Geophys. Res. Lett., 39, L20815, doi:10.1029/2012GL053253, 2012.

World Health Organization. (2009). Global Health Risks: Mortality and Burden of Disease Attributable to Select Major Risks (Geneva, Switzerland: World Health Organization). Available

at: http://www.who.int/healthinfo/global_burden_disease/GlobalHealthRisks_report_full.pdf, last access: 24 April 2017.

Zhang, Q., Jimenez, J. L., Canagaratna, M. R., Allan, J. D., Coe, H., Ulbrich, I., Alfarra, M., Takami, A., Middlebrook, A. M., Sun, Y., Dzepina, K., Dunlea, E., Docherty, K., DeCarlo, P. F., D., S., Onasch, T. B., Jayne, J., Miyoshi, T., Shimono, A., Hatakeyama, S., Takegawa, N., Kondo, Y., Schneider, J., Drewnick, F., Borrmann, S., Weimer, S., Demerjian, K., Williams, P., Bower, K., Bahreini, R., Cottrell, L., Griffin, R. J., Rautiainen, J., Sun, J., Zhang, Y., and Worsnop, D.: Ubiquity and dominance of oxygenated species in organic aerosols in anthropogenically-influenced Northern Hemisphere midlatitudes, Geophys. Res. Lett., 34, L13801, doi:10.1029/2007GL029979, 2007.

Zhang, Q., Jimenez, J. L., Canagaratna, M. R., Ulbrich, I. M., Ng, N. L., Worsnop, D. R., and Sun, Y.: Understanding atmospheric organic aerosols via factor analysis of aerosol mass spectrometry: a review, Anal. Bioanal. Chem., 401, 3045-3067, 2011.

Zhao, D. F., Buchholz, A., Kortner, B., Schlag, P., Rubach, F., Fuchs, H., Kiendler-Scharr, A., Tillmann, R., Wahner, A., Watne, Å K., Hallquist, M., Flores, J. M., Rudich, Y., Kristensen, K., Hansen, A. M. K., Glasius, M., Kourtchev, I., Kalberer, M., and Mentel, Th F.: Cloud condensation nuclei activity, droplet growth kinetics, and hygroscopicity of biogenic and anthropogenic secondary organic aerosol (SOA), Atmos. Chem. Phys., 16, 1105-1121, 2016.

Zhao, D. F., Buchholz, A., Kortner, B., Schlag, P., Rubach, F., Kiendler-Scharr, A., Tillmann, R., Wahner, A., Flores, J. M., Rudich, Y., Watne, Å K., Hallquist, M., Wildt, J., and Mentel, Th F.: Size-dependent hygroscopicity parameter (κ) and chemical composition of secondary organic cloud condensation nuclei, Geophys. Res. Lett., 42, 10920-910928, 2015.

1   **Table 1.** Summary of the hygroscopicity parameters (κ) and material densities of different

2   chemical constituents utilized in the theoretical κ calculation with chemical data.

Chemical compounds	Hygroscopicity parameter, κ	Density (10^3 kg/m^3)
$SNA^{\dagger}$	0.59	1.77
EC	0	1.80
$PBOA$	0.04^{ζ}	1.10
$BBOA$	0.06^{ζ}	1.20
OOA	κ_{OOA}^{*}	1.50
Bulk OA	κ_{org}^{*}	1.40

3   † *SNA* includes all the sulfate, nitrate, and ammonium in submicron wildfire haze particles.

4    $^{\zeta}$ κ values were assumed according to the mean κ results derived from laboratory studies (Chen et

5   al., 2017).

6   * κ_{OOA} and κ_{org} were derived from ambient water uptake measurements and chemical data, in

7   combination of the given parameters in Table 1, using the simplified algorithm introduced in

8   Sects. 3.3 and 3.2.

Table 2. Summary of the averaged chemical characteristics of the 24 h $PM_{2.5}$ filter samples collected during 2015 haze events and the accordingly calculated mean κ results of organics ($RH = 85$ %).

Sampling date	Cl$^-$ ($\mu g/m^3$)	NO$_3^-$ ($\mu g/m^3$)	SO$_4^{2-}$ ($\mu g/m^3$)	Na$^+$ ($\mu g/m^3$)	NH$_4^+$ ($\mu g/m^3$)	K$^+$ ($\mu g/m^3$)	Mg^{2+} ($\mu g/m^3$)	Ca^{2+} ($\mu g/m^3$)
Oct-14	0.64	2.40	10.21	0.20	4.93	0.62	0.05	0.55
Oct-15	0.38	1.72	10.51	0.18	4.63	0.60	0.03	0.50
Oct-16	0.27	1.62	9.01	0.25	4.03	0.48	0.08	0.65
Oct-19	0.65	2.39	15.90	0.20	7.99	0.58	0.03	0.41
Oct-20	0.24	1.09	10.22	0.31	4.33	0.51	0.05	0.48
Oct-21	0.19	0.83	7.95	0.23	3.15	0.51	0.08	0.52
Oct-22	0.23	0.80	9.71	0.29	3.78	0.38	0.08	0.50
Oct-23	0.56	2.65	15.92	0.18	9.13	0.70	0.005	0.25
Average	0.40	1.69	11.18	0.23	5.25	0.55	0.05	0.48

Sampling date	f_{inorg}* (%)	f_{SO4}^{2-} (%)	f_{EC} (%)	WSOC/OC (%)	Mean κ	Mean κ_{org}[†] ($D_0 = 100$ nm)	Mean κ_{OOA}[†]
Oct-14	42.1	21.9	15.3	79.9	0.114	0.030	0.054
Oct-15	41.1	23.3	11.1	64.8	0.202	0.118	0.185
Oct-16	28.6	15.7	11.7	66.4	0.161	0.133	0.256
Oct-19	26.6	15.0	5.9	60.2	0.265	0.229	0.450
Oct-20	30.3	18.0	11.3	61.5	0.271	0.236	0.443
Oct-21	26.4	15.6	11.0	56.9	0.193	0.148	0.283

Oct-22	42.9	26.4	15.8	59.5	0.265	0.212	0.376
Oct-23	24.6	13.3	4.4	59.6	0.217	0.184	0.337
Average	30.5	17.2	10.8	63.6	0.211	0.161	0.298

1   * The subscript $_{inorg}$ stands for all the inorganic species; hence, f_{inorg} is the mass fraction of

2   inorganic particles in the $PM_{2.5}$ filter sample. All the ionic data are provided with the mean mass

3   concentration ($\mu g/m^3$).

4   [†] The mean κ results of organics were calculated assuming 10.0 % elemental carbon (EC) in total

5   mass (see Sect.3.2).

1 **Table 3.** Derived mean κ values of organics with consideration of 10.0 % *EC* mass fraction in

2 total NR-PM$_1$, as well as the mean κ results for HTDMA measurements conducted within the

3 overlapped ToF-ACSM observation period of 10−24 October 2015 (i.e., κ_{HTDMA}).

	Mean κ (mean ± SD)		
	Overall	**Daytime**	**Nighttime**
κ_{org}	0.157 ± 0.108	0.200 ± 0.104	0.103 ± 0.086
κ_{OOA}	0.266 ± 0.184	0.323 ± 0.177	0.186 ± 0.177
κ_{HTDMA}	0.207 ± 0.093	0.247 ± 0.096	0.160 ± 0.063

1   **Table 4.** The temporally mean number fraction (*nf*), volume-weighted mean diameter growth

2   factor (*GF*), and κ results (mean ± SD) of 100 nm wildfire haze particles in the three different

3   hygroscopicity ranges at 85 % *RH*.

Hygroscopic mode	*nf*	*GF*	κ
Weakly ($g < 1.15$)	0.42 ± 0.18	1.05 ± 0.02	0.030 ± 0.013
Moderately ($1.15 \leq g < 1.27$)	0.18 ± 0.07	1.21 ± 0.01	0.151 ± 0.005
More ($1.27 \leq g < 1.85$)	0.40 ± 0.20	1.40 ± 0.05	0.343 ± 0.054
Bulk mean	*n/a*	1.25 ± 0.09	0.189 ± 0.087

4   *n/a*: not applicable.
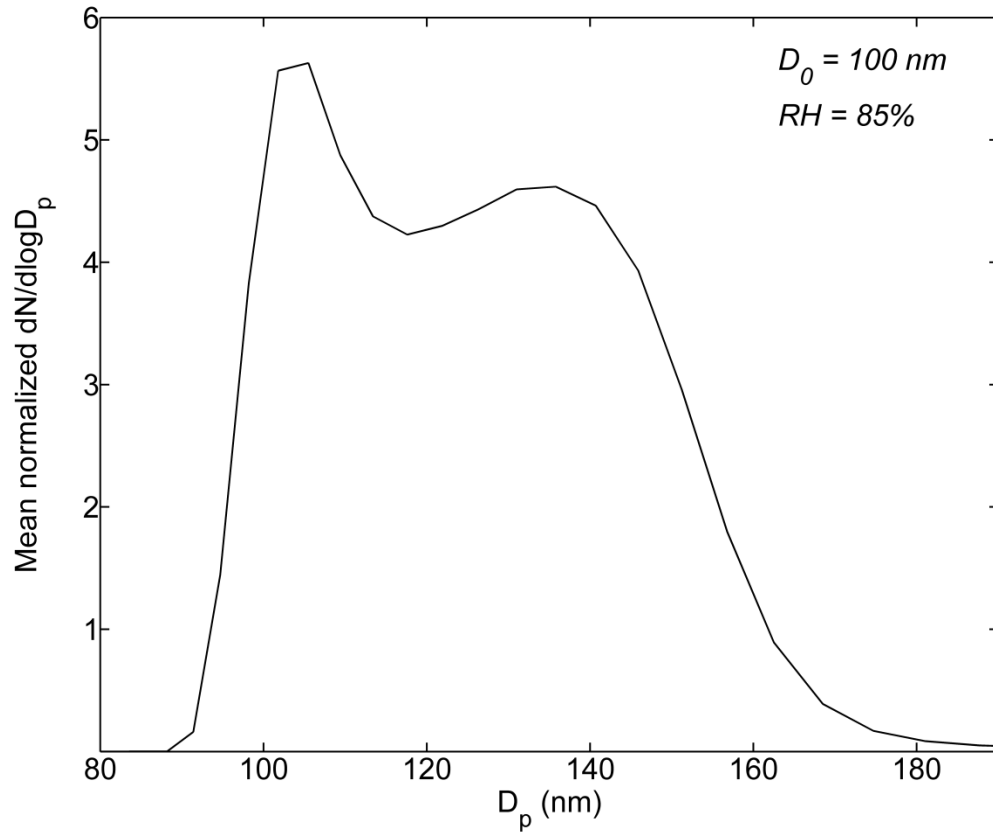
2   **Fig. 1** Normalized particle number size distribution ((dN/dlogDp)/N) after humidification

3   averaged over the entire haze observation period.
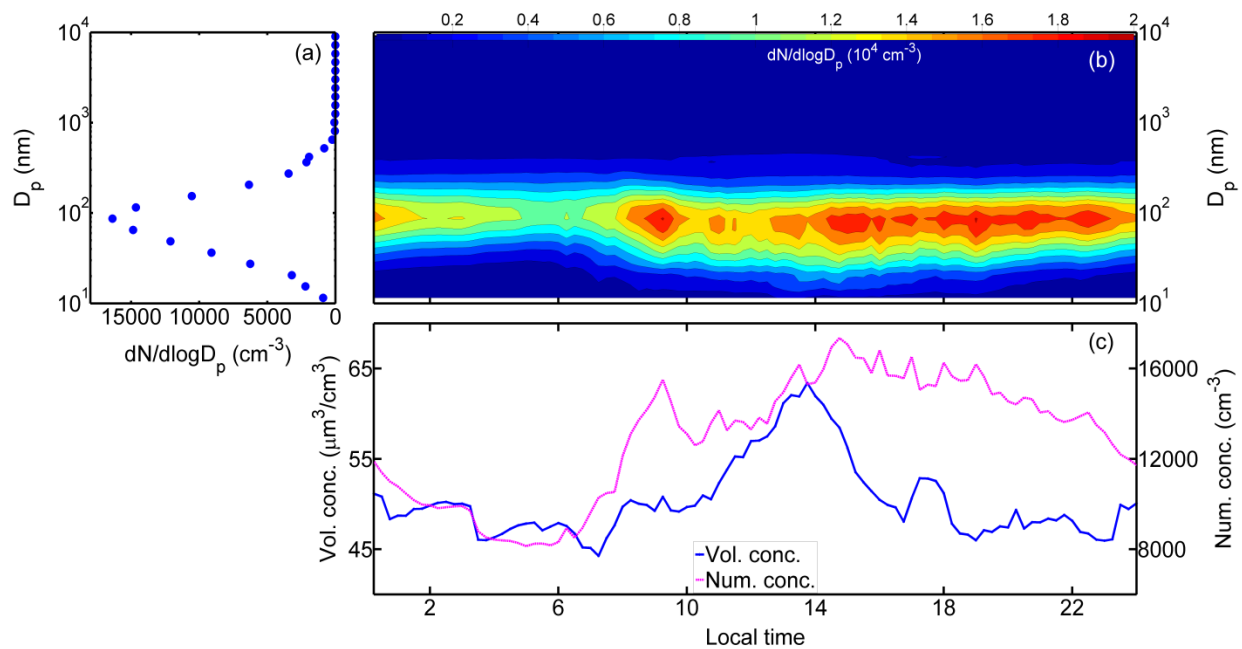
Fig. 2 (a) The mean particle number size distribution (dN/dlogD$_p$, cm^{-3}) during the ambient wildfire haze observations as well as the mean diurnal variations of (b) particle size distribution, (c) number concentration (Num. conc., cm^{-3}, denoted by the magenta solid line), and volume concentration (Vol. conc., μm^3/cm^3, as the blue line displayed) measured with NanoScan-SMPS (11.5−365.2 nm) and OPS (419 nm–10 μm) (local time, LT).

High aerosol loading was commonly observed during the transboundary wildfire haze. Submicron particles in the size range of 30−200 nm dominated the total number concentration of wildfire haze particles.
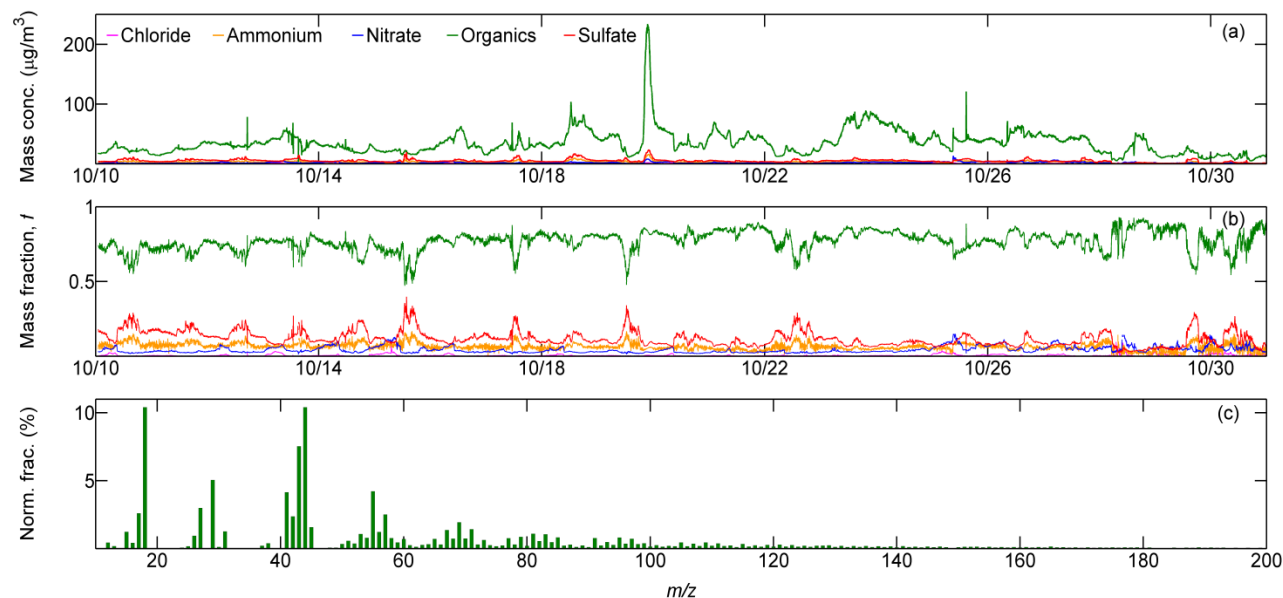
Fig. 3 Time series of (a) mass concentration (Mass conc., μg/m³) and (b) corresponding mass fraction, *f*, of the five specific chemical species in NR-PM$_1$ measured by ToF-ACSM (abscissa shows the observation dates in October 2015 in the date format of month/day). (c) Temporally averaged OA mass spectra for submicron wildfire haze particles, displayed with the normalized ion fraction (Norm. frac., %) of each ion fragment.

Wildfire haze particles were predominantly composed of organics. Ion signals (*m/z*) from oxygenated organics (e.g., *m/z* 43, 44) were prominent, while intensities of ions for hydrocarbon-like organic compounds (e.g., *m/z* 41, 55, 57) and biomass burning tracers (e.g., *m/z* 60, 73) were relatively less intense. See the text for details.
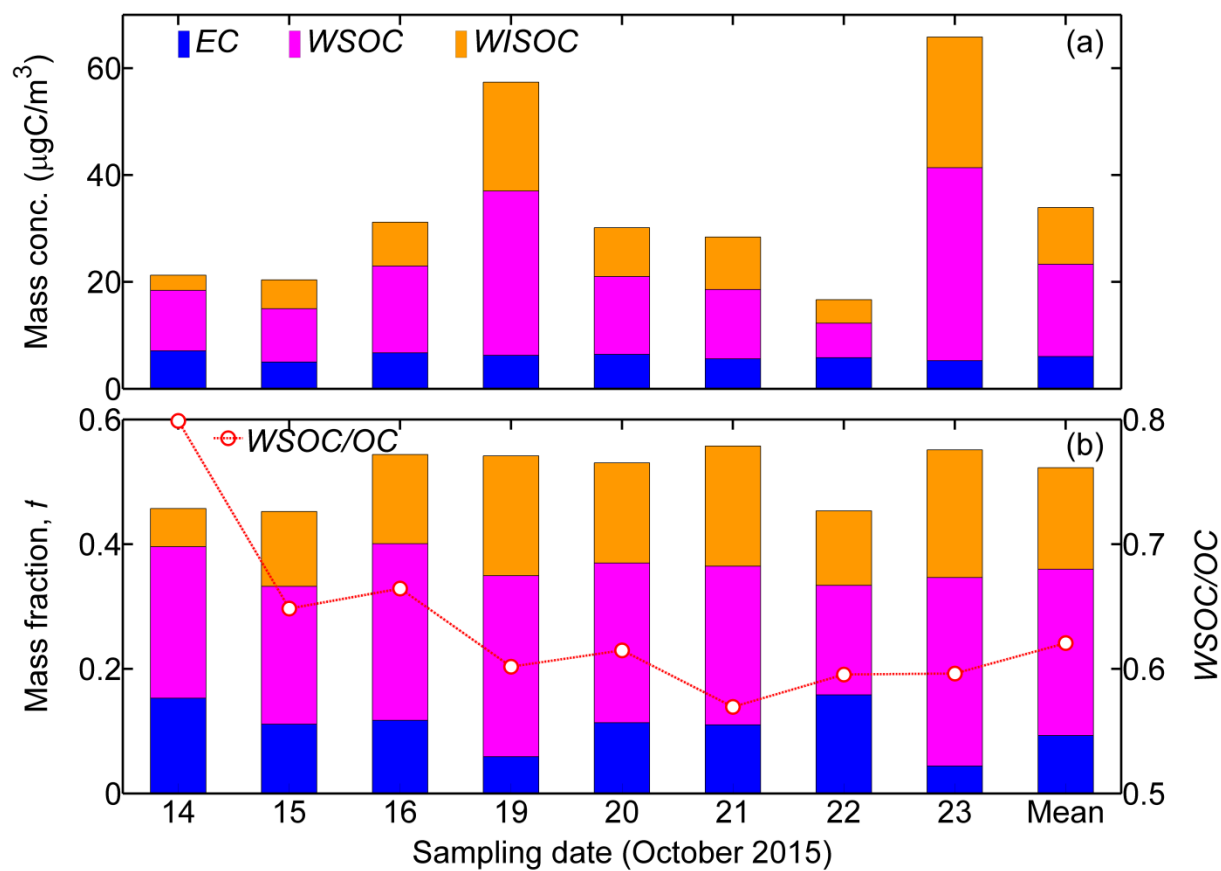
Fig. 4 (a) Mass concentration (Mass conc., μgC/m³) and (b) corresponding mass fraction, *f*, of the carbon contents including *EC*, *WSOC*, and water-insoluble *OC* (*WISOC*) in *PM*$_{2.5}$ filter samples. The *WSOC/OC* ratio is also displayed by the scattered dots in panel (b). All the corresponding temporal mean results are shown as "Mean".

The *WSOC* fraction was exclusively higher than that of *WISOC* or *EC*, highlighting the dominance of *WSOC* in the carbon content of *PM*$_{2.5}$ filter samples. In general, the *EC* fraction fluctuated around 10.0 % of the total *PM*$_{2.5}$ mass.
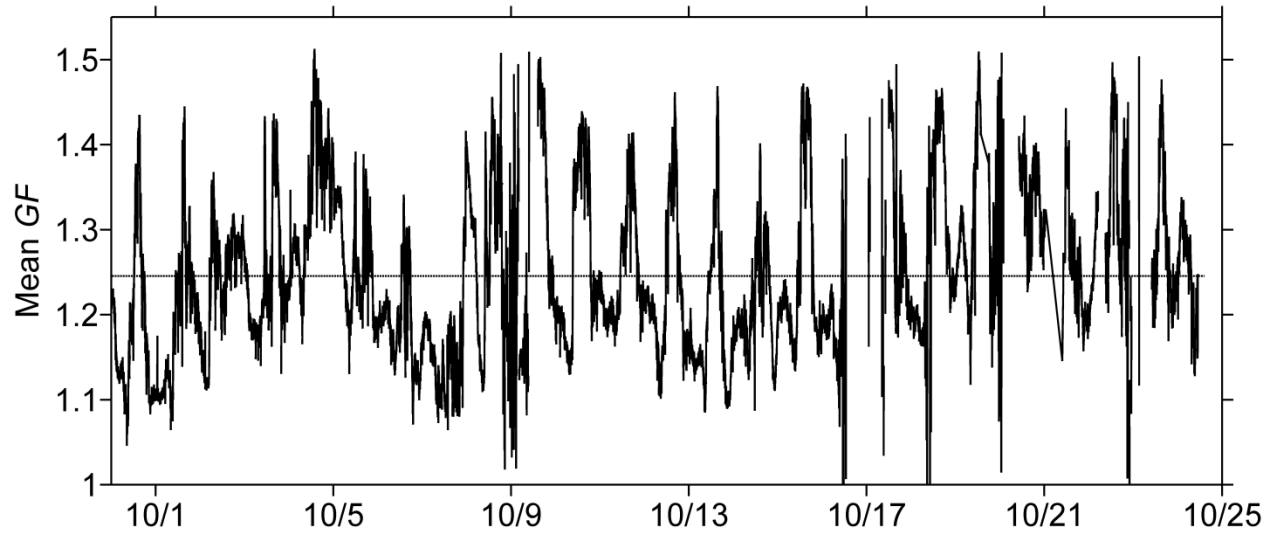
3 **Fig. 5** Time series of the volume-weighted mean particle diameter growth factor (*GF*) derived

4 from HTDMA measurements (date format: month/day, 2015). The black dashed line stands for

5 the temporal mean *GF* averaged over the entire observation period.
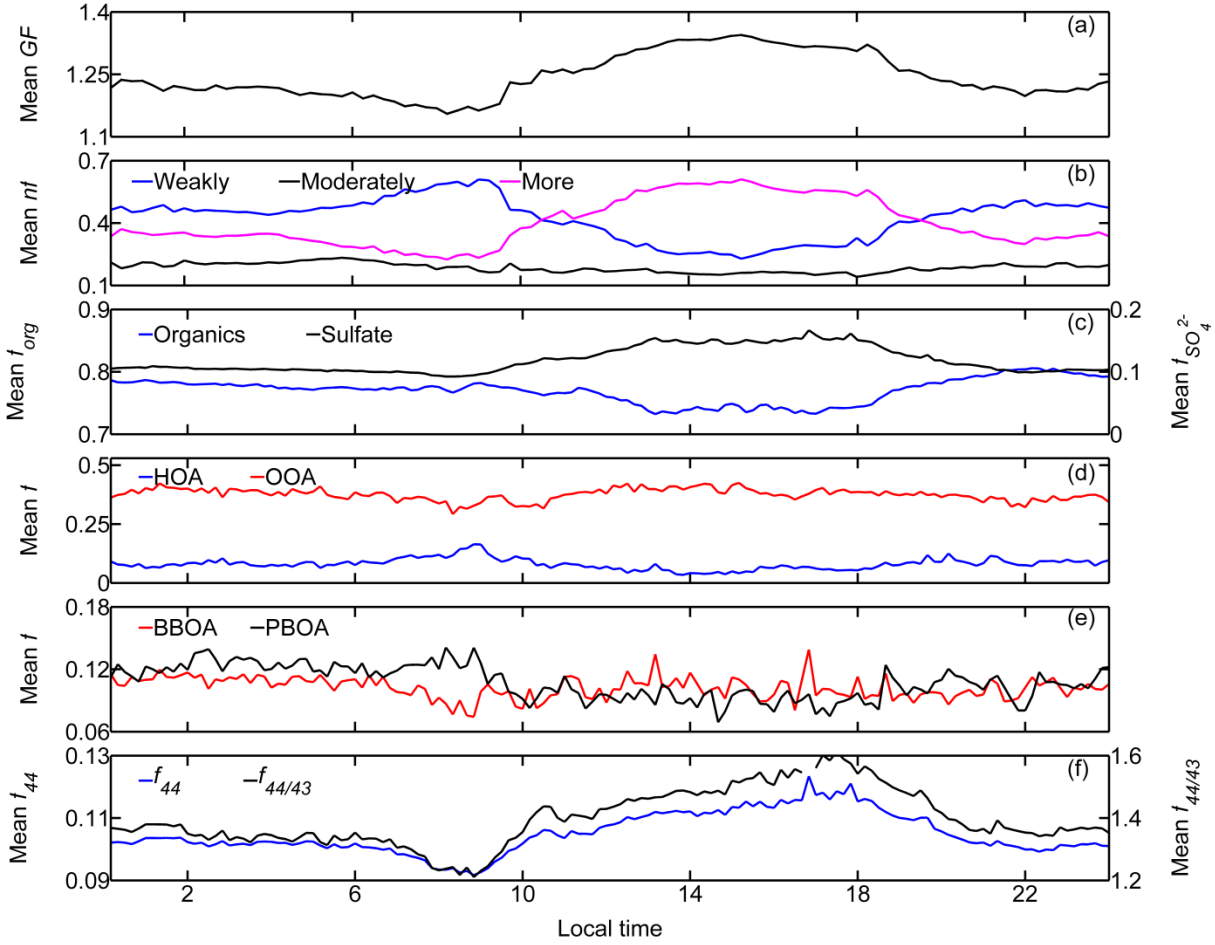
Fig. 6 Temporal averaged (10−24 October 2015) diurnal variations of (a) the mean *GF*, (b) number fraction (*nf*) of the three hygroscopic modes, (c) mass fraction of the two main components in NR-PM$_1$, i.e., organics (f_{org}) and sulfate ($f_{SO_4^{2-}}$), (d-e) mass fraction of the ME2-resolved four OA factors in NR-PM$_1$ (i.e., f_{HOA}, f_{OOA}, f_{BBOA}, and f_{PBOA}), and (f) mean f_{44} and $f_{44/43}$ of organics in NR-PM$_1$ (local time, LT).

Pronounced diurnal patterns were observed for the mean *GF*, number fractions of both weakly and more hygroscopic modes, f_{44}, $f_{44/43}$, and mass fractions of organics and sulfate as well as HOA and OOA; nf_{more}, $f_{SO_4^{2-}}$, f_{44}, $f_{44/43}$, and f_{OOA} showed variations similar to that of the mean *GF*, whereas contrasting diurnal patterns were found for nf_{weakly}, f_{org}, and f_{HOA}.
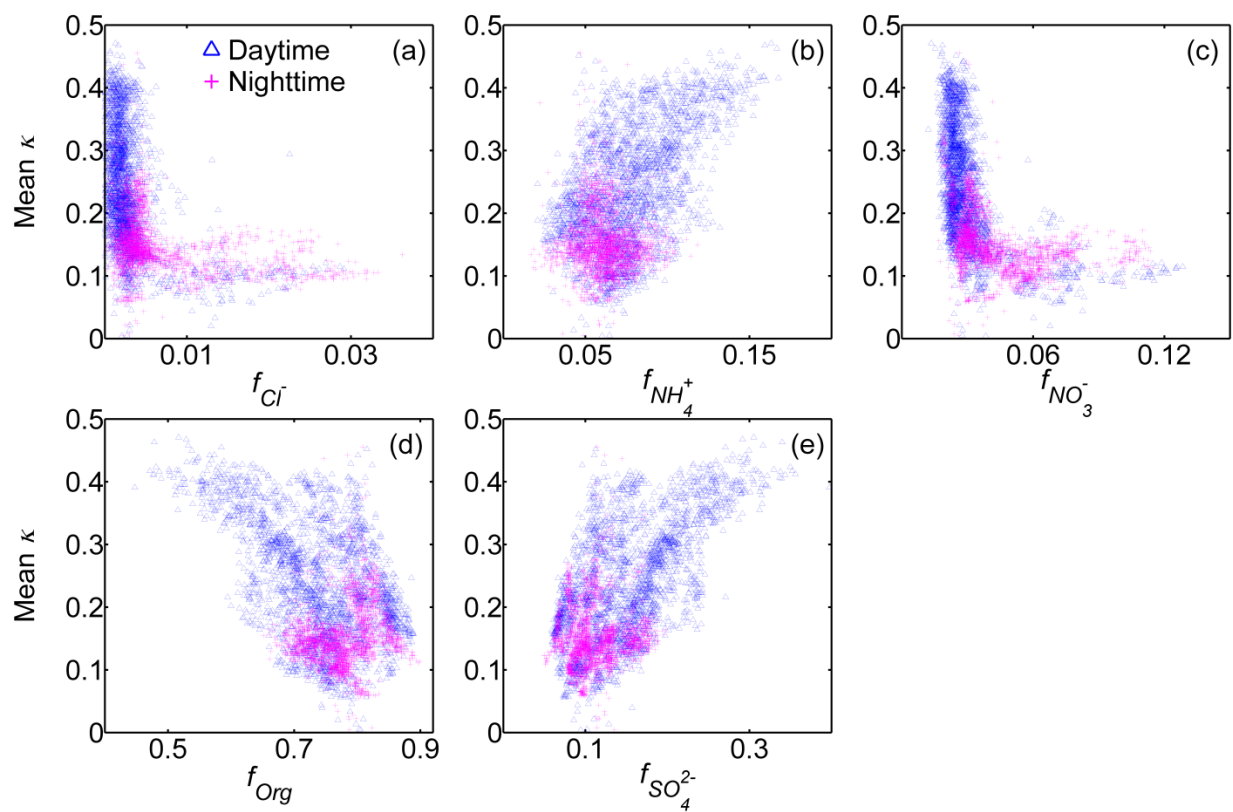
Fig. 7 Relationships between the mean κ results (100 nm) and the mass fractions of the five non-refractory chemical compositions of submicron wildfire haze particles.
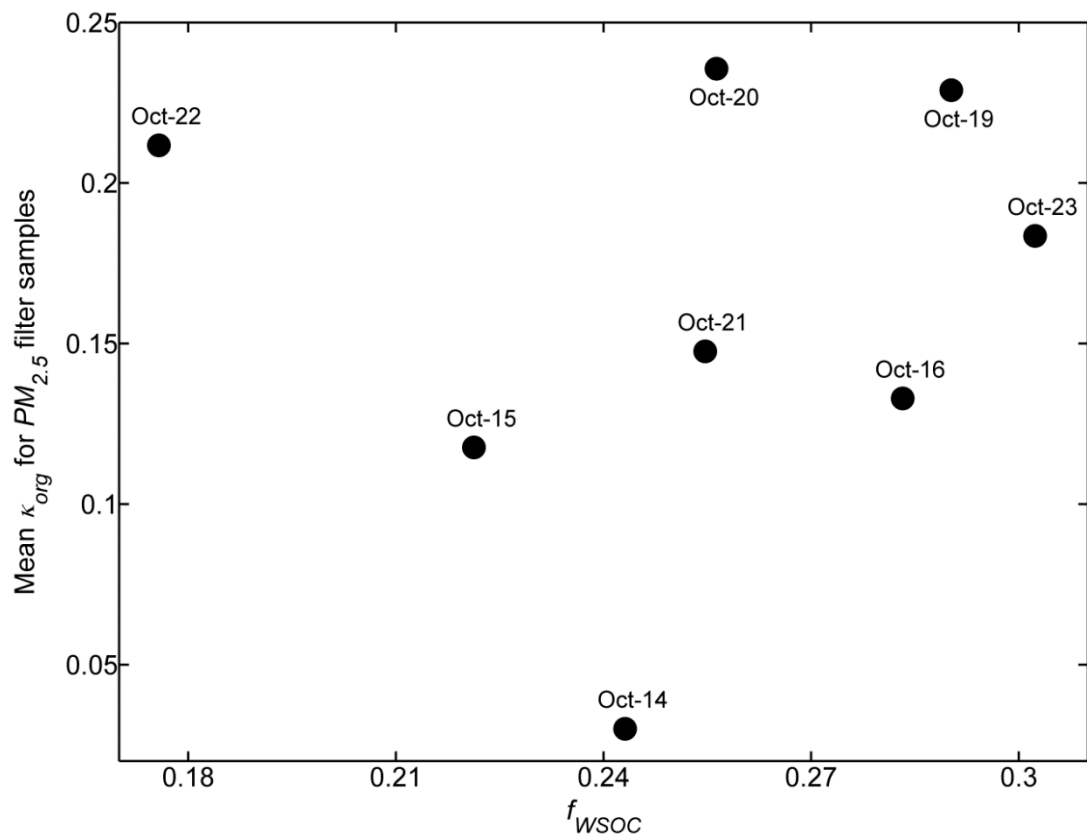
2   **Fig. 8** Correlation between the mean κ of organics (κ_{org}, with 10.0 % *EC* mass fraction

3   considered in the κ calculation) and the mean *WSOC* fraction (f_{WSOC}) of *PM$_{2.5}$* filter samples.
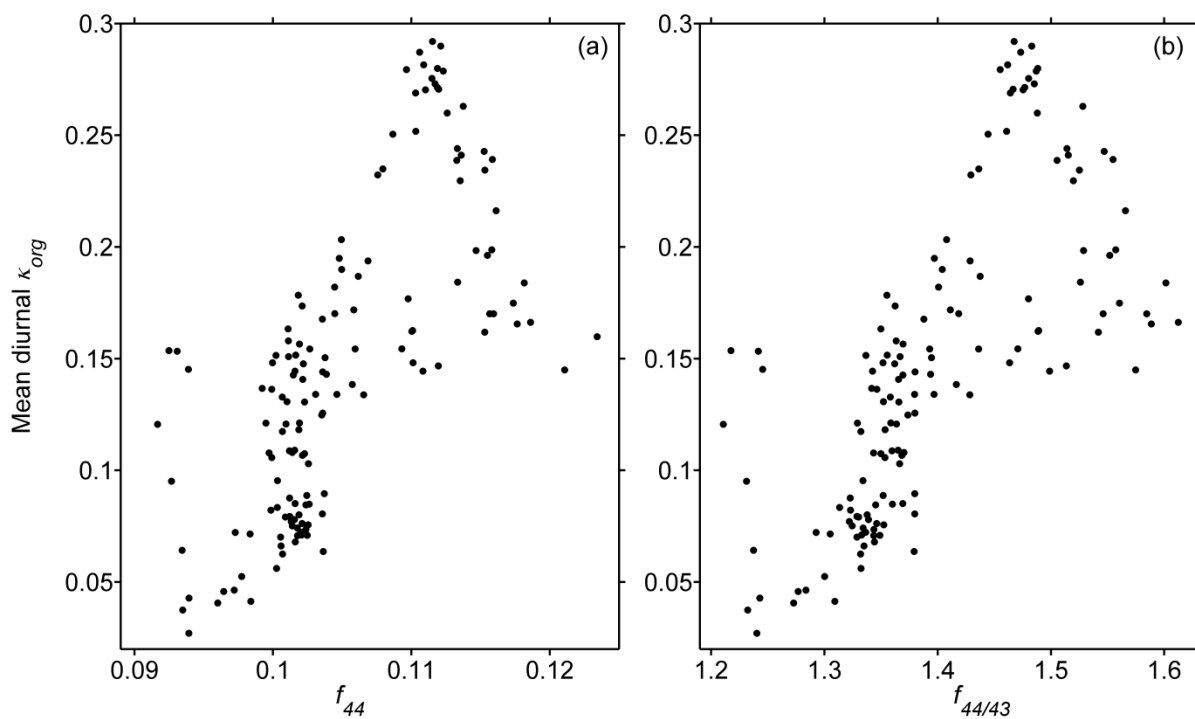
Fig. 9 Relationships between the mean diurnal κ_{org} results vs. (a) f_{44} and (b) $f_{44/43}$ in NR-PM$_1$ haze particles. Mean diurnal here represents that the diurnal results for each day were further averaged over the overlapping observation period, i.e., with both HTDMA and ToF-ACSM measurements taken from 10−24 October 2015.